Fundamentals and applications of coherent microwave scattering

Alexey Shashurin
School of Aeronautics and Astronautics, Purdue University

Purdue University | School of Aeronautics and Astronautics, College of Engineering

Online Low Temperature Plasma (OLTP) seminar
January 24, 2023

Team

- Dr. Alexey Shashurin, Dr. Mikhail Slipchenko, Dr. Sergey Macheret (Purdue University)
- Dr. Mikhail Shneider (Princeton University)
- Dr. Andrius Baltuska, Dr. Audrius Pugzlys, Dr. Valentina Shumakova (TU Wien, Austria)
- PhD students:
    - Adam Patel, Xingxing Wang, Animesh Sharma, Apoorv Ranjan, Nick Babusis, Won Joon Jeong (Aero. and Astro. Eng., Purdue)
    - Erik Braun, K. Arafat Rahman, (Mech. Eng., Purdue)
    - Chris Galea (Mech. and Aero. Eng., Princeton University)

Electric Propulsion and Plasma Laboratory (EPPL)

- Nanosecond repetitively pulsed discharges
- Laser-induced plasmas
- Microwave/optical diagnostics for combustion and electric propulsion
- Electric propulsion systems for CubeSats
- High power microwave gas heating
- Generation, diagnostics and applications of cold plasmas

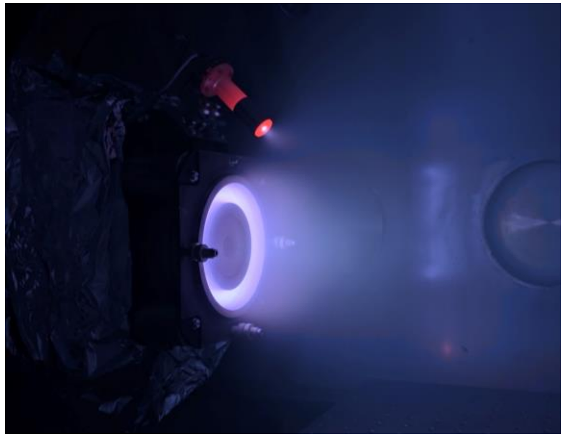
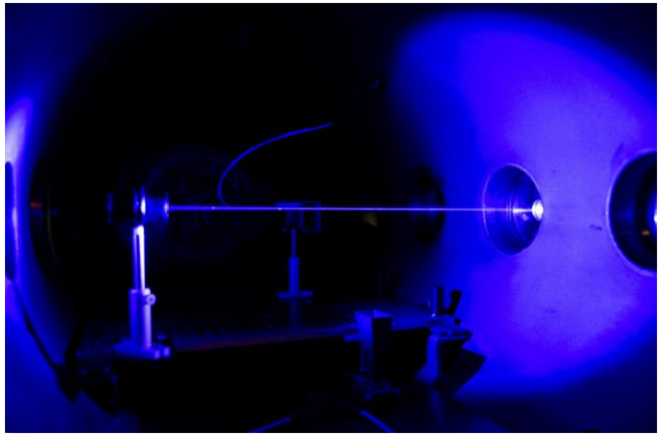
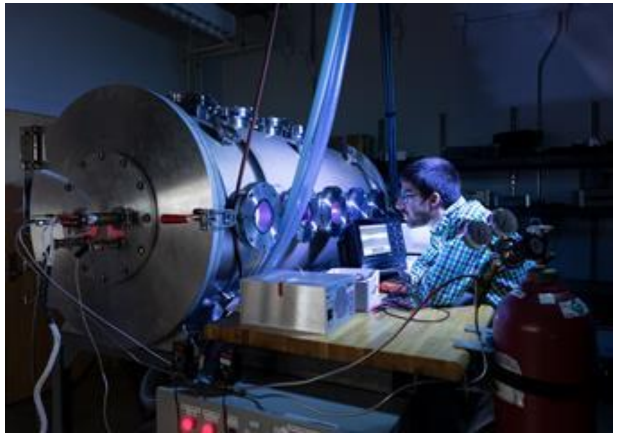
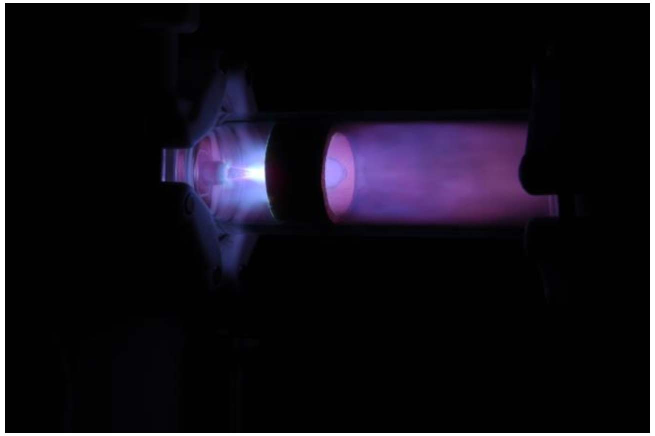
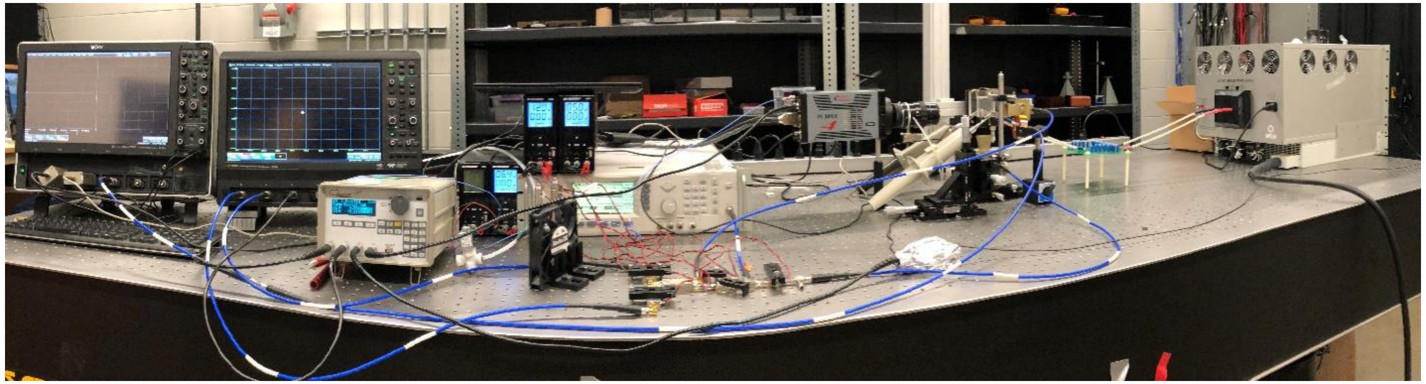
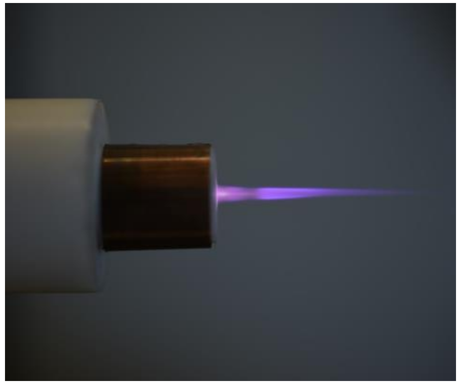
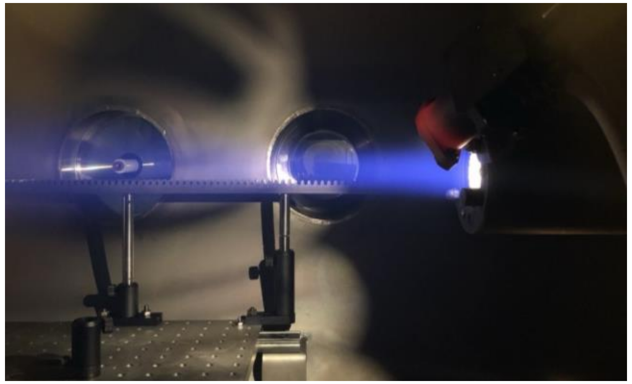

Outlook

1. Coherent Microwave Scattering (CMS):
   - Fundamentals and Experimental Implementation
   - Experimental Validation of the Scattering Regimes
2. Plasma dynamics and electron decay
   - Laser induced plasmas
   - Nanosecond repetitively pulsed discharges
   - Small plasma objects enclosed within glass tubes
3. Photoionization rates
   - Femtosecond photoionization at 800nm and 3.9 um
4. Electron Momentum Transfer Collision Frequency
5. Diagnostics of selective species in gaseous mixtures
   - Electric Propulsion applications
   - Combustion applications
6. Conclusions

Scattering in optical frequency range

Rayleigh scattering

Bound electrons (Lorentz oscillator model): $\omega_0 \gg \omega$

$$\ddot{s} + \omega_0^2 s = -\frac{e}{m} E_0 \cos(\omega t)$$ - restoring force dominates

$\ddot{s} \sim \omega^2 s$

$$\omega_0^2 s = -\frac{e}{m} E_0 \cos(\omega t)$$

$$\ddot{s}^2 \propto \omega^4 \; (P_{rad} \propto \ddot{d}^2 \propto \ddot{s}^2)$$

$$\sigma \propto \langle \ddot{s}^2 \rangle \propto \omega^4 \propto \frac{1}{\lambda^4}$$ - classical Rayleigh cross-section

Rayleigh scattering of light:

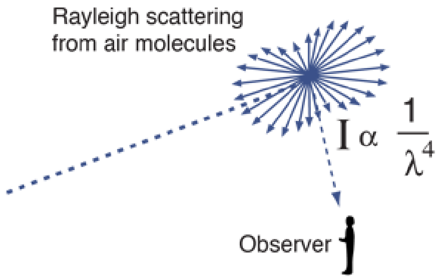

Characteristic spatial scale: ~100s of nm

>>

Particle size

(Otherwise, Mie scattering)

Reproduced from http://hyperphysics.phy-astr.gsu.edu/

Thomson scattering

Free electrons:

$$\ddot{s} + \omega_0^2 s = -\frac{e}{m} E_0 \cos(\omega t)$$ - no restoring force

$$\ddot{s} = -\frac{e}{m} E_0 \cos(\omega t)$$

$\ddot{s}^2$ – independent of $\omega \Rightarrow \sigma \propto \langle \ddot{s}^2 \rangle$ – independent of ω

$$\sigma_T = \frac{8\pi}{3}\left(\frac{e^2}{4\pi\varepsilon_0 m c^2}\right)^2$$ - Thomson cross-section

Thomson scattering on plasma electrons:

- Incoherent: n_e (>10^{10} cm^{-3}) and T_e measurements
- Coherent: Waves, dispersion relations

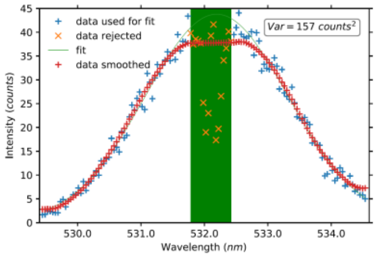

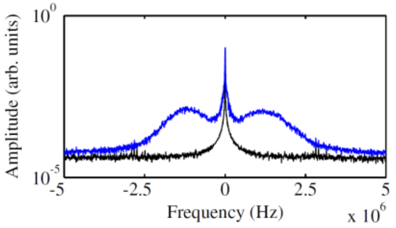

Tsikata et al. 2015, 2018

Scattering off small-size plasmas in microwave frequency range (Shneider & Miles 2005)

Wavelength: large compared to the optical band (e.g., λ =3 cm for 10 GHz)

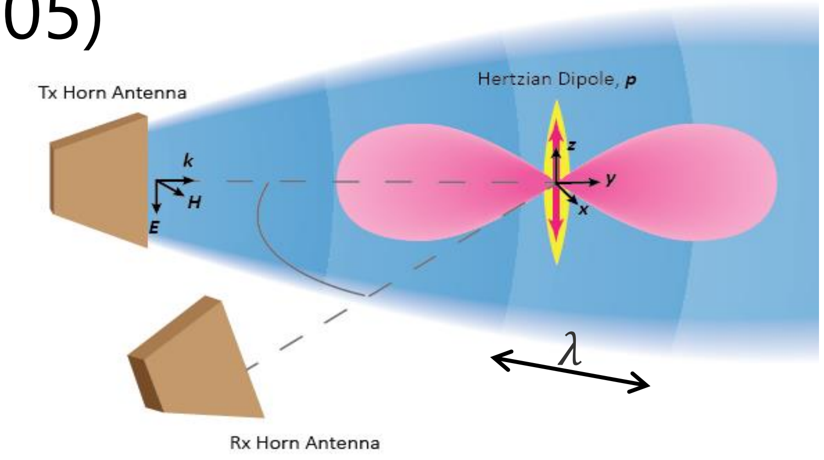

Small plasma size (< λ):

- Entire plasma volume "sees" the same phase of incident field
- Detector is nearly equidistant from each plasma element

Scattered power:

$$\langle \frac{dP_S}{dA} \rangle = c\varepsilon_0 \langle \sum_{j=1}^{N} \boldsymbol{E}_{jS} \cdot \sum_{l=1}^{N} \boldsymbol{E}_{lS} \rangle = \frac{c\varepsilon_0}{2} N E_{S,0}^2 + c\varepsilon_0 \langle \sum_{\substack{j,l=1 \\ l \neq j}}^{N} \boldsymbol{E}_{jS} \cdot \boldsymbol{E}_{lS} \rangle$$

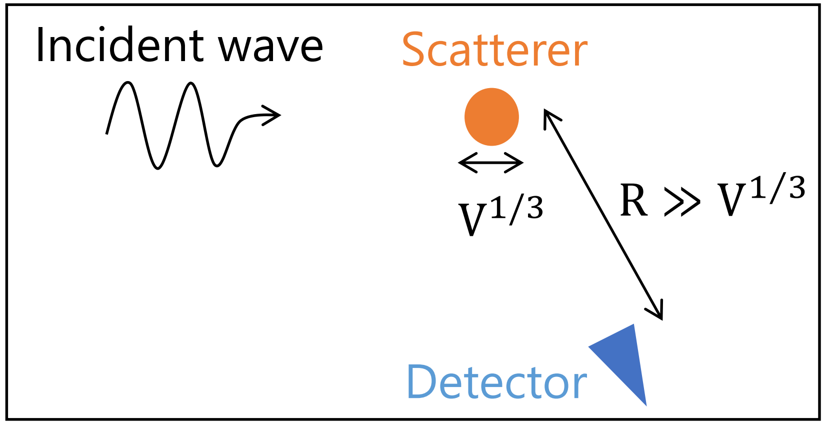

- $\langle \frac{dP_S}{dA} \rangle$ - time-averaged scattered power per unit area at detector location
- $\boldsymbol{E}_{jS}$ - field by jth electron at observation location
- $E_{S,0}$ - field amplitude at observation location (same by each electron)

In-phase coherent scattering:

$$\langle \frac{dP_S}{dA} \rangle = c\varepsilon_0 \langle \underbrace{\sum_{j=1}^{N} \boldsymbol{E}_{jS}}_{N\boldsymbol{E}_{jS}} \cdot \underbrace{\sum_{l=1}^{N} \boldsymbol{E}_{lS}}_{N\boldsymbol{E}_{jS}} \rangle = \frac{c\varepsilon_0}{2} N^2 E_{S,0}^2$$

The Fluid-Short Dipole Formulation

Consider scattering from linear, unmagnetized short plasma dipole:

L - plasma length
D - plasma diameter

Skin depth $\delta \gg D$
Wavelength $\lambda \gg D, L$

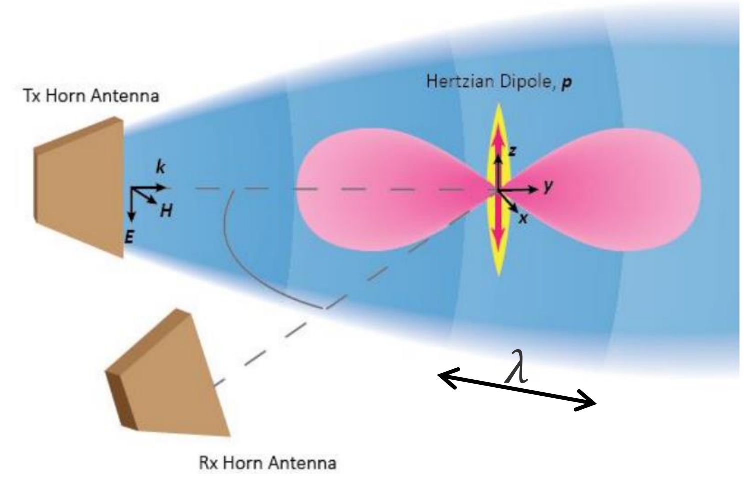

Collisions are not negligible: $\nu_m \sim 10^9 \cdot p$(Torr) ~ 10^{10} Hz (for 10 Torr)
Microwave frequency ~10 GHz → $\omega \sim 6 \times 10^{10}$ s^{-1}

Equation of motion for the electron swarm in a linearly-polarized incident plane wave (Lorentz oscillator):

$$\ddot{s} + \nu_m \dot{s} = -\frac{e}{m} E$$

Electric field inside plasma:

$$E = E_I + E_{dep}$$

E_I - incident irradiating field
E_{dep} - depolarizing field
E - total electric field inside the plasma volume

Apply complex formalism $(E_I = E_{I,0}\cos(\omega t) = Re\{\tilde{E}_{I,0} e^{i\omega t}\};\ s = s_0 \cos(\omega t + \Phi) = Re\{\tilde{s}_0 e^{i\omega t}\})$**:**

$$\ddot{s} + \nu_m \dot{s} + \xi \omega_p^2 s = -\frac{e}{m} E_I$$

$$\tilde{E}_0 = \frac{\tilde{E}_{I,0}}{1 + \xi(\tilde{\varepsilon} - 1)}$$

ξ - depolarization factor

$\tilde{\varepsilon} = \varepsilon' - i\varepsilon'' = \left(1 - \frac{\omega_p^2}{\omega^2 + \nu_m^2}\right) - i \frac{\omega_p^2}{\omega^2 + \nu_m^2} \frac{\nu_m}{\omega}$ - dielectric permittivity

$\omega_p = \sqrt{\frac{n_e e^2}{m \varepsilon_0}}$ - plasma frequency

Solving through complex formalism for phase and amplitude of oscillations:

- Displacement Amplitude: $s_0 = |\tilde{s}_0| = \frac{e}{m} \frac{E_{I,0}}{\sqrt{\left(\xi \omega_p^2 - \omega^2\right)^2 + (\nu_m \omega)^2}}$
- Phase: $\tan(\Phi) = \frac{-\nu_m \omega}{\xi \omega_p^2 - \omega^2}$ (phase-lag between the electron displacement and the incident electric field)
- Dipole Moment: $d_0 = e s_0 \int n_e(r,z) 2\pi r dr dz = e s_0 N_e = \frac{e^2}{m} \frac{E_{I,0}}{\sqrt{\left(\xi \omega_p^2 - \omega^2\right)^2 + (\nu_m \omega)^2}} N_e$

PURDUE UNIVERSITY

The Fluid-Short Dipole Formulation (continued)

Time-Averaged Scattered Power: $P_S = \frac{\ddot{\mathbf{d}}^2}{6\pi\varepsilon_0 c^3} \rightarrow \langle P_S \rangle = \frac{\omega^4 d_0^2}{12\pi\varepsilon_0 c^3} = \frac{e^4}{6\pi m^2 \varepsilon_0^2 c^4} \frac{I_I \omega^4}{\left(\xi\omega_p^2 - \omega^2\right)^2 + (\nu_m \omega)^2} N_e^2$

Total-Cross Section: $\sigma_{Tot} = \frac{\langle P_S \rangle}{I_I} = \sigma_{Th} \frac{\omega^4}{\left(\xi\omega_p^2 - \omega^2\right)^2 + (\nu_m\omega)^2} N_e^2 = \sigma_e N_e^2$

$\sigma_{Th} = \frac{e^4}{6\pi m^2 \varepsilon_0^2 c^4}$ - Thomson cross-section

Differential Cross-Section:

$$\frac{d\sigma_{Tot}}{d\Omega} = \frac{3}{8\pi} \sigma_{Tot} \sin^2(\theta)$$

$$\frac{dP_S}{d\Omega} = \frac{d\sigma_{Tot}}{d\Omega} I_I$$

Phase: $\tan(\Phi) = \frac{-\nu_m \omega}{\xi\omega_p^2 - \omega^2}$

Most common scenario ($\xi\omega_p^2$ is negligible):

- Frequency ~10 GHz → $\omega \sim 6 \times 10^{10}$ rad/s
- For p=760 Torr→ $\nu_m \sim 10^{12}\text{s}^{-1}$ → $\nu_m >> \omega$ (Collisional)
- For p=1 Torr→ $\nu_m \sim 10^9\text{s}^{-1}$ → $\omega >> \nu_m$ (Thomson)

Scattering regimes:

$$\ddot{s} + \nu_m \dot{s} + \xi\omega_p^2 s = -\frac{e}{m} E_I$$

Regime	Condition	Coherent scattering cross-section, σ_e	Phase shift, Φ
Thomson	$\omega^2 \gg \nu_m\omega, \xi\omega_p^2$	σ_{Th}	0°
Collisional	$\nu_m\omega \gg \left\lvert\xi\omega_p^2 - \omega^2\right\rvert$	$\sigma_{Th}\left(\frac{\omega}{\nu_m}\right)^2 \propto \frac{1}{\lambda^2}$	90°
Rayleigh	$\xi\omega_p^2 \gg \omega^2, \nu_m\omega$	$\sigma_{Th}\left(\frac{\omega^2}{\xi\omega_p^2}\right)^2 \propto \frac{1}{\lambda^4}$	180°

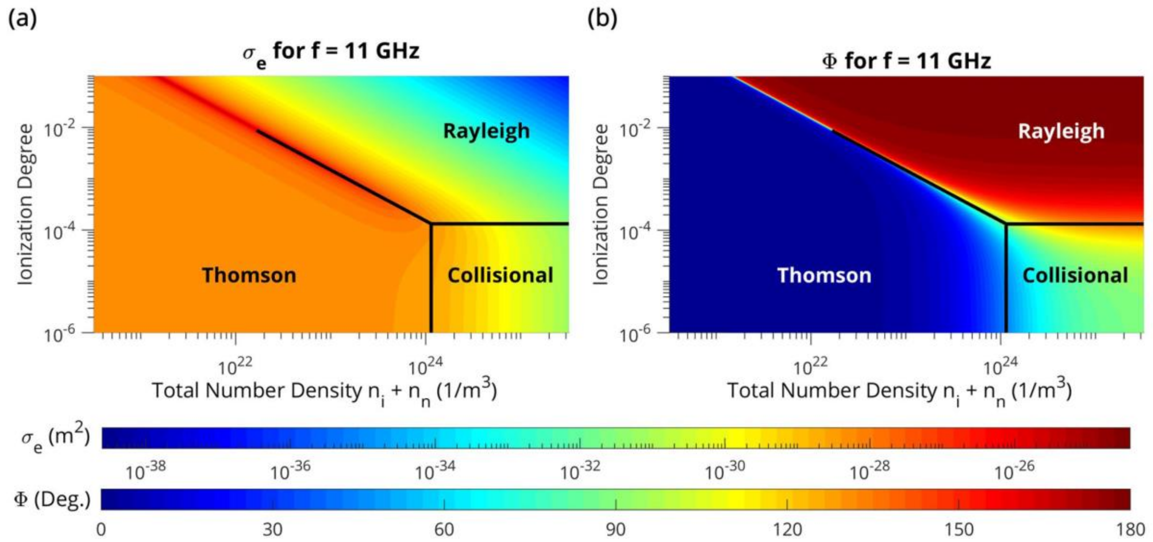

Experimental Implementation

Microwave scattering detection system (based on I/Q mixer):

$$I = \frac{\kappa B_{LO}}{2}\eta B_B\, cos(\Phi_B) + \frac{\kappa B_{LO}}{2}\eta B_S\, cos\big(\Phi_S(t)\big) = V_{\bar{I},0} + \Delta V_{\bar{I}}$$

$$Q = \frac{\kappa B_{LO}}{2}\eta B_B\, sin(\Phi_B) + \frac{\kappa B_{LO}}{2}\eta B_S\, sin\big(\Phi_S(t)\big) = V_{\bar{Q},0} + \Delta V_{\bar{Q}}$$

$$\boxed{V_S = \sqrt{\Delta V_{\bar{I}}^2 + \Delta V_{\bar{Q}}^2} \propto B_S \propto E_{S,0};\;\; \Phi_S = \tan^{-1}\big(\Delta V_{\bar{Q}}/\Delta V_{\bar{I}}\big)}$$

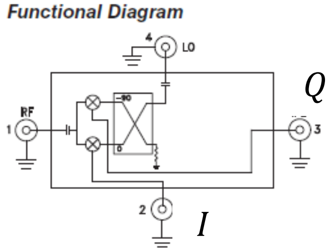

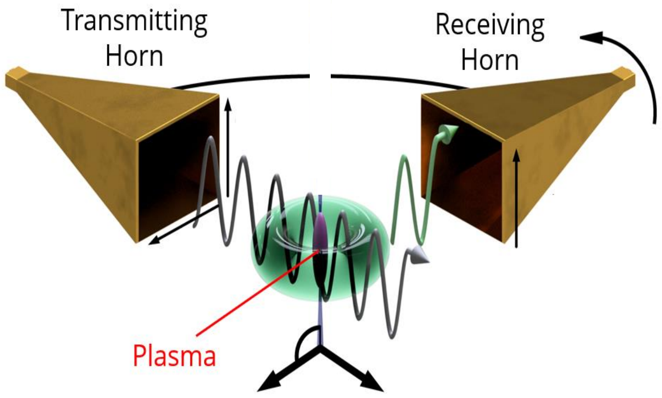

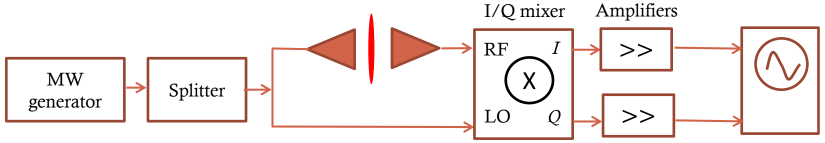

Electron Number Measurements:

- $V_S \propto E_{S,0}|\cos(\beta)| = \sqrt{\frac{3\langle P_S\rangle}{4\pi\varepsilon_0 c}}\frac{|\sin(\theta)\cos(\beta)|}{R} = \frac{e^2\omega^2 E_{I,0}}{4\pi R m\varepsilon_0 c^2}\frac{|sin(\theta)\cos(\beta)|}{\sqrt{\left(\xi\omega_p^2-\omega^2\right)^2+(\nu_m\omega)^2}}N_e$
- For prolate plasma ellipsoids (ξ << 1) with moderate electron number densities: $\xi\omega_p^2$ is negligible
- Math for dielectric scatterers: $\sigma_{Tot,D} = \frac{\langle P_S\rangle}{I_I}$; $\sigma_{Tot,D} = \frac{\omega^2}{6\pi\varepsilon_0^2 c^4}\left(\varepsilon_0(\varepsilon_D - 1)\omega V_D\right)^2$

Plug-in A → Determine N_e

Measure → $V_S = \begin{cases} A\dfrac{e^2}{m\sqrt{\omega^2+\nu_m^2}}N_e & -\text{ plasma scatterer} \\ AV_D\varepsilon_0(\varepsilon_D - 1)\omega & -\text{ dielectric scatterer}\end{cases}$ → $n_e = \dfrac{N_e}{V_p}$

Determine A

Photography

Phase measurements:

- Φ_S → Φ → $\tan(\Phi) = \dfrac{\nu_m}{\omega}$

Sensitivity and temporal resolution

CMS sensitivity:

- Sensitivity is governed by N_e: $\langle P_S \rangle = \sigma_{Th} \frac{\omega^4}{\left(\xi\omega_p^2-\omega^2\right)^2+(\nu_m\omega)^2} N_e^2\, I_I$
- High sensitivity due to in-phase coherency: $\langle P_S \rangle \propto N_e^2$ (not $\langle P_S \rangle \propto N_e$ as for incoherent counterpart)
- Minimal measurable N_e ~10^7 electrons (currently)
- Measurements down to n_e ~10^{12} cm^2 are feasible
- Single-shot measurements

Temporal resolution:

- Several periods of incident microwave radiation
- < 1 ns

Ways to improve sensitivity:

$$V_S \propto E_{S,0}|\cos(\beta)| = \frac{e^2\omega^2 E_{I,0}}{4\pi R m \varepsilon_0 c^2} \frac{|sin(\theta)\cos(\beta)|}{\sqrt{\left(\xi\omega_p^2-\omega^2\right)^2+(\nu_m\omega)^2}} N_e$$

- Increase amplitude of incident MW field, but keeping it non-intrusive
- Decrease distance to horn, but keeping it in far-field
- Increase sensitivity of MW detection system, e.g. homodyne and heterodyne detection schemes
- Increase probing frequency (collisional regime): up to about 250 GHz for 100 um plasma channels

Outlook

1. Coherent Microwave Scattering (CMS):
   - Fundamentals and Experimental Implementation
   - Experimental Validation of the Scattering Regimes
2. Plasma dynamics and electron decay
   - Laser induced plasmas
   - Nanosecond repetitively pulsed discharges
   - Small plasma objects enclosed within glass tubes
3. Photoionization rates
   - Femtosecond photoionization at 800nm and 3.9 um
4. Electron Momentum Transfer Collision Frequency
5. Diagnostics of selective species in gaseous mixtures
   - Electric Propulsion applications
   - Combustion applications
6. Conclusions

Experimental Validation of the Thomson and Collisional Regimes

Collisional vs. Thomson regimes:

Regime	Condition	Coherent scattering cross-section, σ_e	Phase Shift, Φ
Thomson	$\omega \gg \nu_m$	σ_{Th}	0°
Collisional	$\nu_m \gg \omega$	$\sigma_{Th}\left(\frac{\omega}{\nu_m}\right)^2 \propto \frac{1}{\lambda^2}$	90°

- Frequency~10 GHz → $\omega \sim 6 \times 10^{10}$ rad/s
- Thomson: p=1 Torr→ $\nu_m \sim 10^9 s^{-1}$ → $\omega >> \nu_m$
- Collisional: p=760 Torr→ $\nu_m \sim 10^{12} s^{-1}$ → $\nu_m >> \omega$
- $\xi \omega_p^2$ is negligible

Phase measurements:

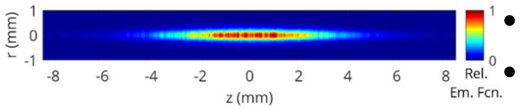

- Laser-induced plasma: 1-760 Torr
- CMS at 11 GHz

$$\tan(\Phi) = \frac{\nu_m}{\omega}$$

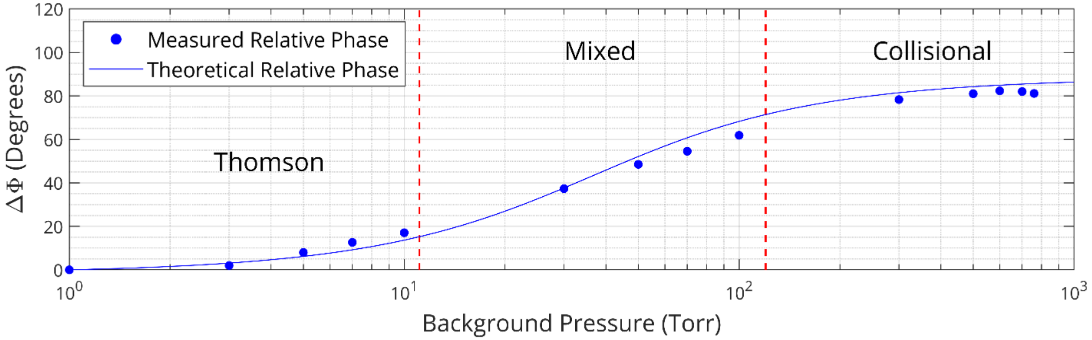

- A 90-degree phase shift is observed as the pressure decreases (transition from Collisional to Thomson)
- The measured phase shift confirms the Thomson scattering regime at low pressures

Scattering cross-section and n_e measurements:

- Glow discharge: Diam-1.5 cm, ~1 Torr
- CMS at 3-4 GHz

$$V_S = A\frac{e^2}{m\omega}N_e$$

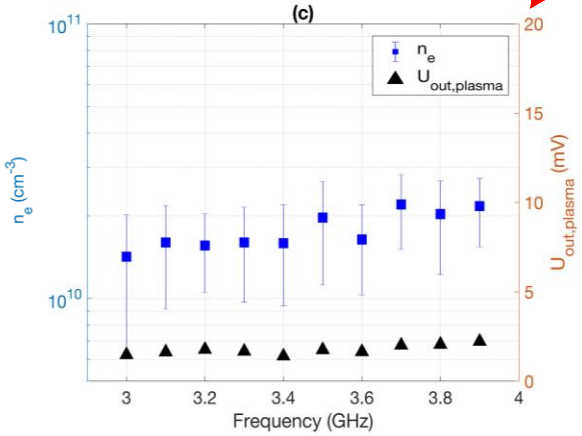

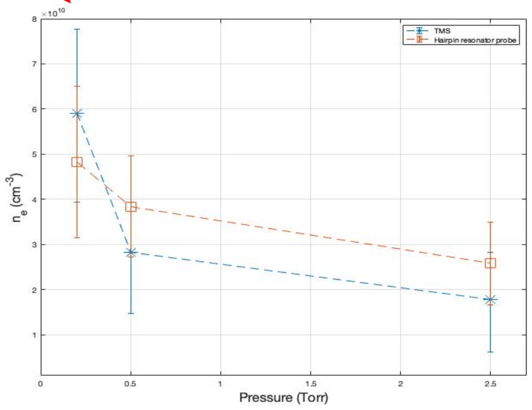

- Scattered signal (cross-section) is independent of frequency: confirms the Thomson scattering regime (unlike $1/\lambda^2$ or $1/\lambda^4$)
- Reasonable agreement between TMS and Hairpin probe

Patel et al. *Sci. Reports* (2021); Ranjan et al. *Rev. Sci. Instrum.* (2022)

Outlook

1. Coherent Microwave Scattering (CMS):
    - Fundamentals and Experimental Implementation
    - Experimental Validation of the Scattering Regimes
2. Plasma dynamics and electron decay
    - Laser induced plasmas
    - Nanosecond repetitively pulsed discharges
    - Small plasma objects enclosed within glass tubes
3. Photoionization rates
    - Femtosecond photoionization at 800nm and 3.9 um
4. Electron Momentum Transfer Collision Frequency
5. Diagnostics of selective species in gaseous mixtures
    - Electric Propulsion applications
    - Combustion applications
6. Conclusions

Laser-induced plasmas

Applications:

- Laser-assisted ignition
- Plasma filamentation physics
- Combustion diagnostics

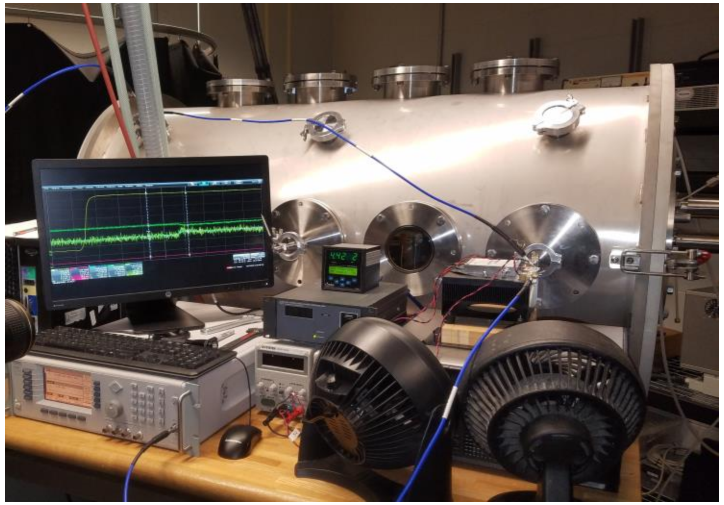

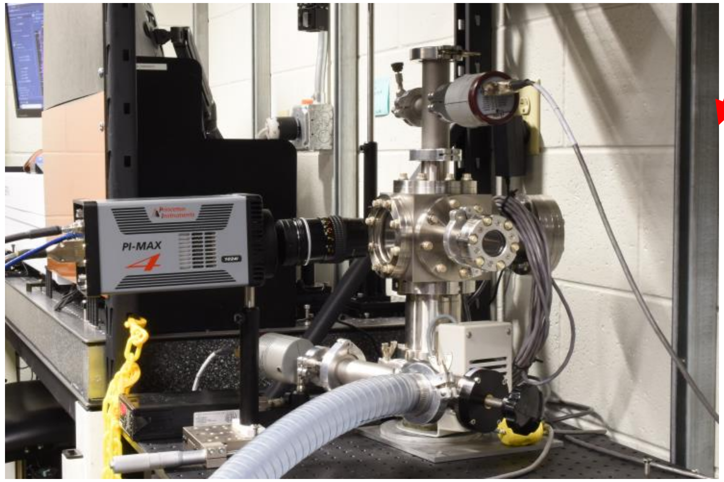

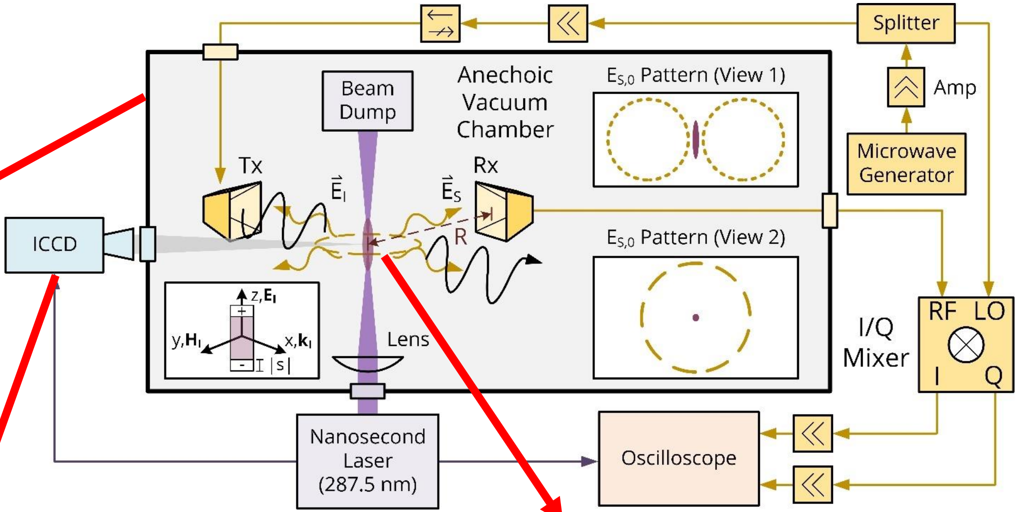

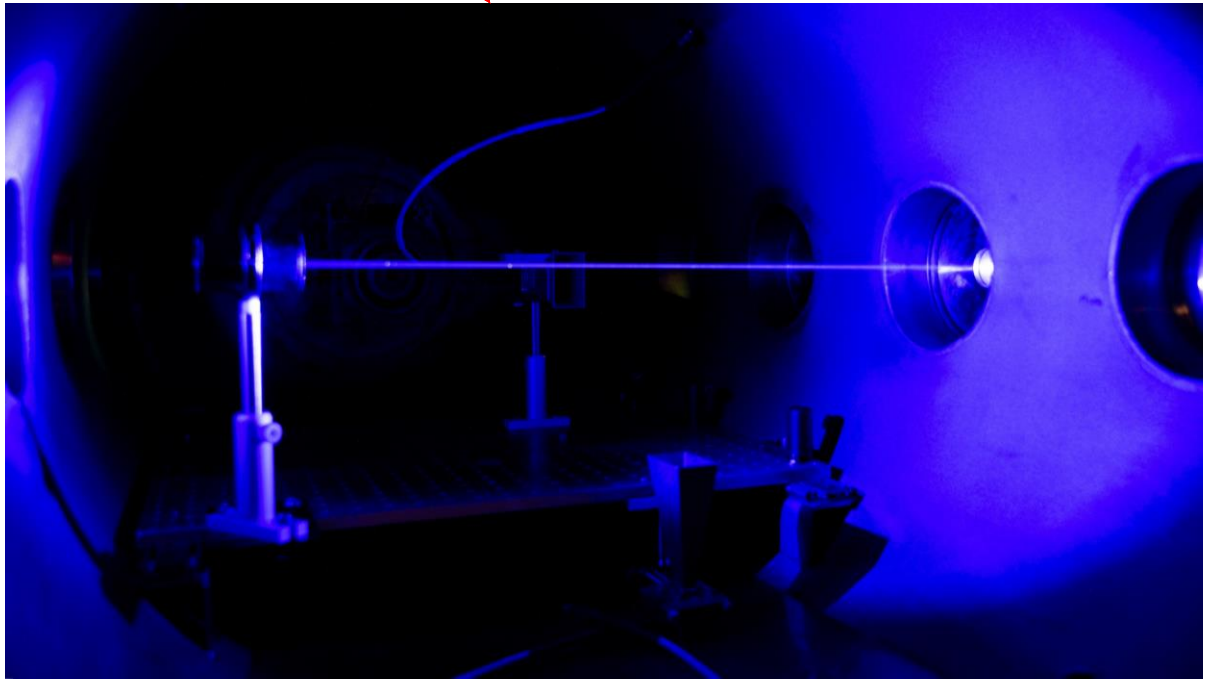

- Laser:
  - 100 fs, <7 mJ, 800nm, 400 mm lens;
  - 5 ns, < 3 mJ, 287.5 nm (2 + 1) REMPI of O2, 175 mm lens;
- CMS: 11 GHz
- Pressure: 1-760 Torr

ICCD Imaging and Radiation Pattern

ICCD Imaging

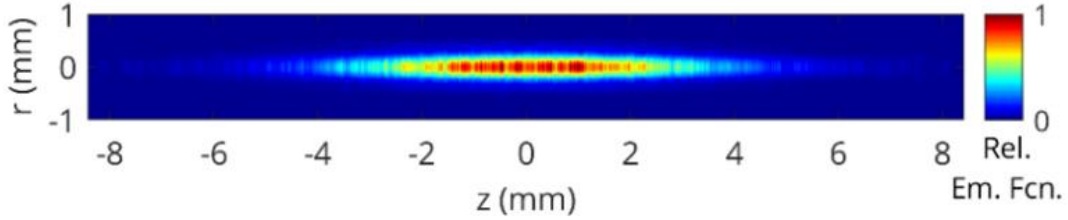

760 Torr; 100 ns, 250 accumulations; Abel Inverted;
$\mathfrak{a} = \mathfrak{b} = 280$ µm, $\mathfrak{c} = 4.5$ mm ($\xi < 0.01$).

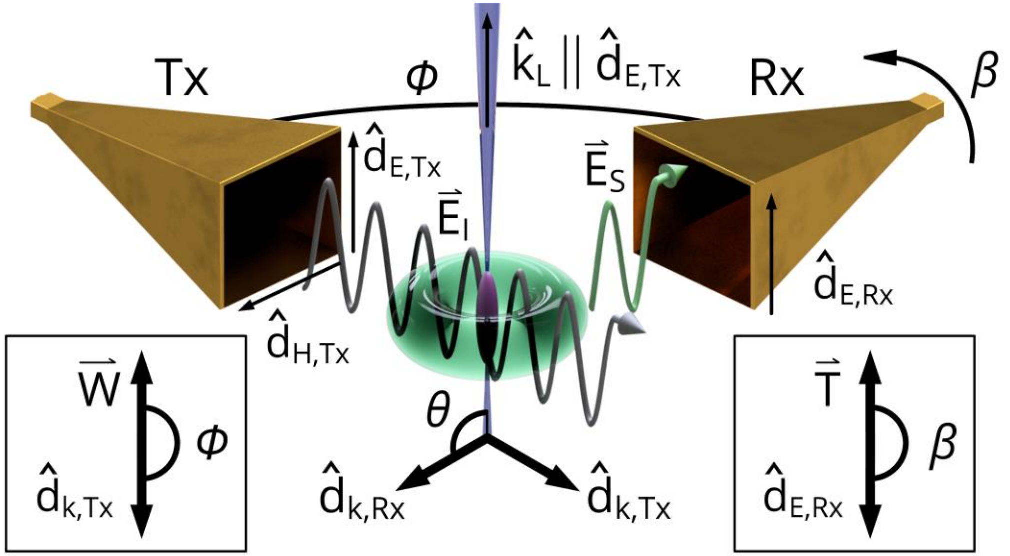

Radiation Pattern

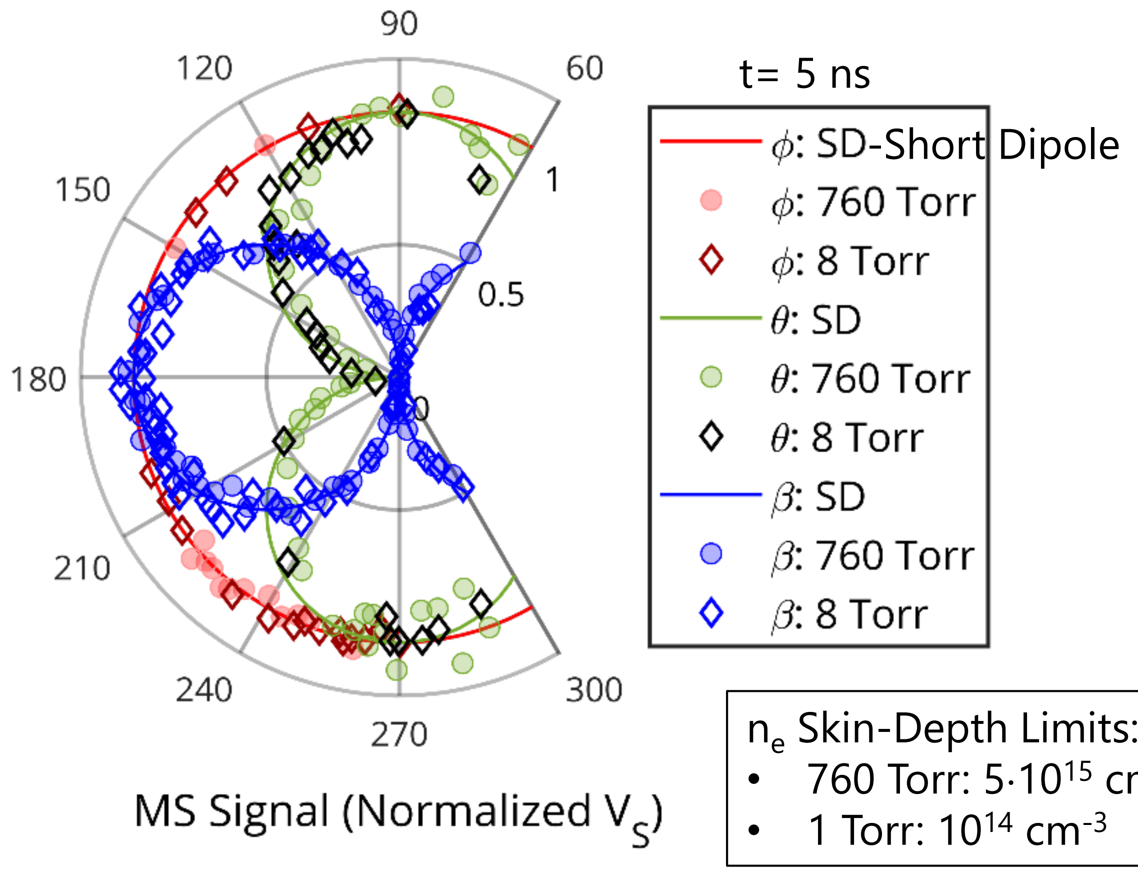

n_e Skin-Depth Limits:
- 760 Torr: $5 \cdot 10^{15}$ cm^{-3}
- 1 Torr: 10^{14} cm^{-3}

- Good agreement between the measured radiation pattern and the theoretical short dipole pattern.

Electron decay in laser-induced plasmas (1 atm, 800 nm)

Electron Decay in air:

Experiment

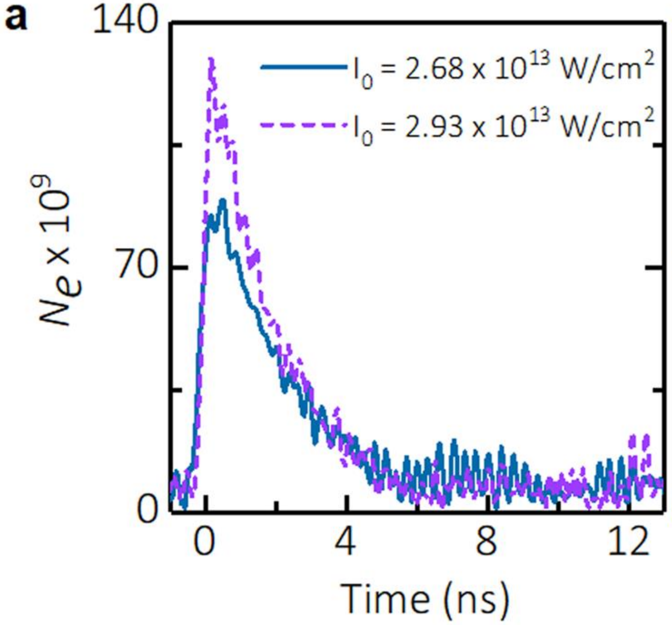

Numerical simulations

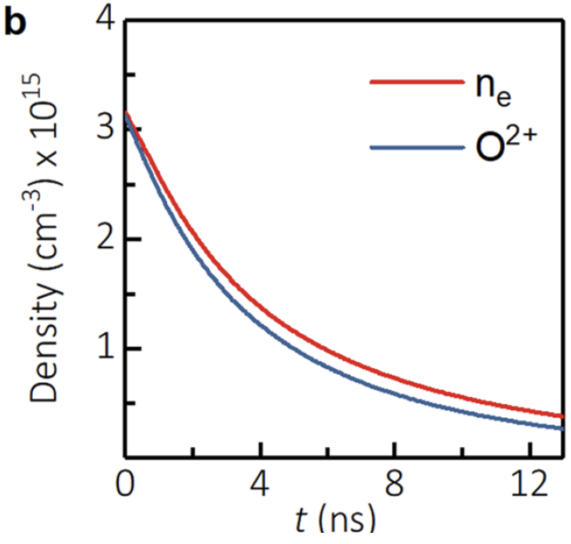

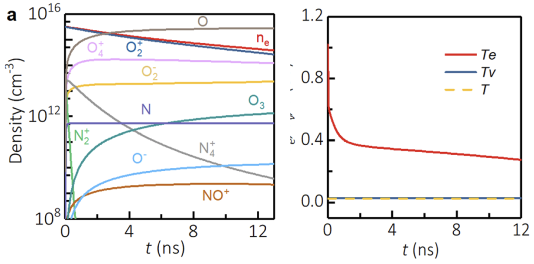

- Analysis of mechanisms of electron decay (e.g., dissociative recombination, attachment to oxygen)
- Validation of numerical codes

Electron Decay in various gases:

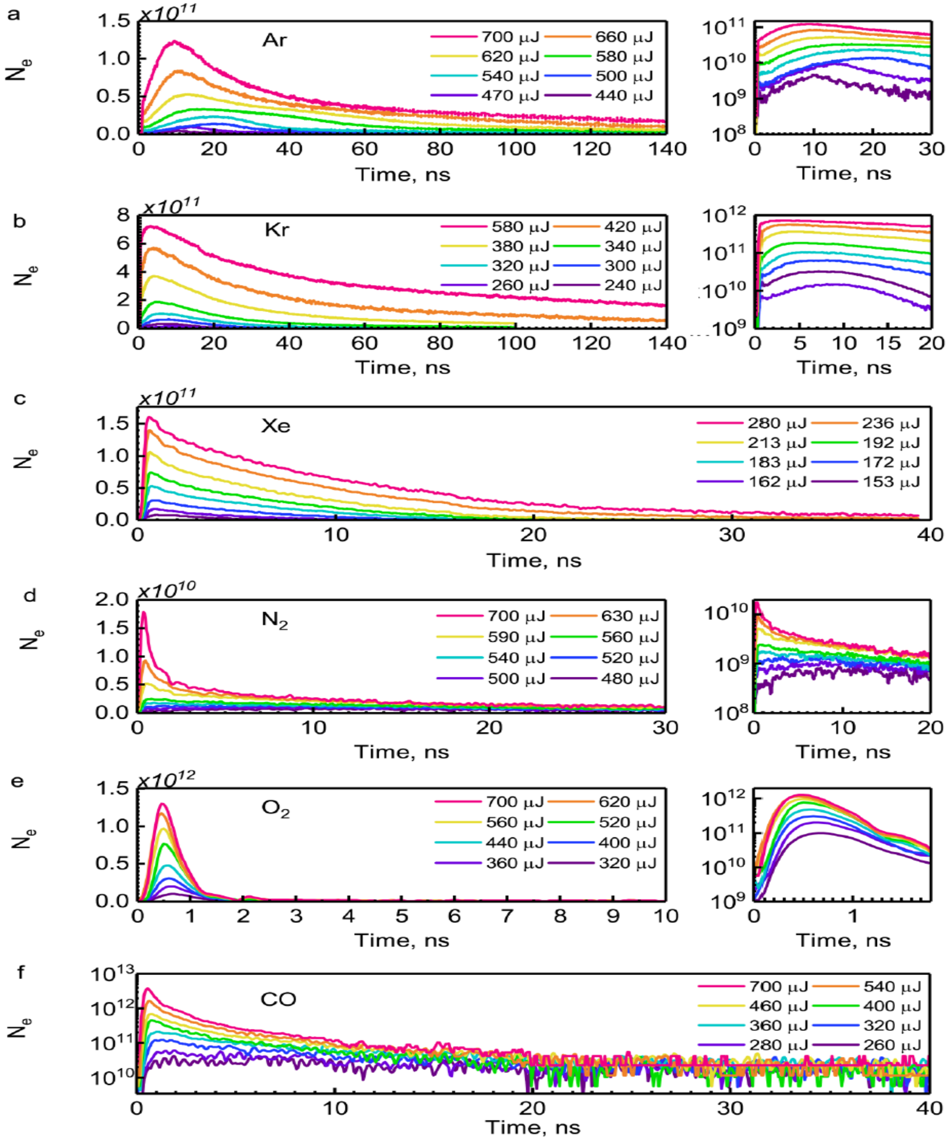

Sharma et.al. *Sci. Reports* (2018); Sharma et.al. *J. Appl. Phys* (2019)

Electron decay in laser-induced plasmas (1-760 Torr, (2+1) REMPI 287.5 nm)

N_e measurements:

$$V_S = \begin{cases} A\dfrac{e^2}{m\sqrt{\omega^2+\nu_m^2}}N_e & -\text{ plasma scatterer} \\ AV_D\varepsilon_0(\varepsilon_D-1)\omega & -\text{ dielectric scatterer} \end{cases}$$

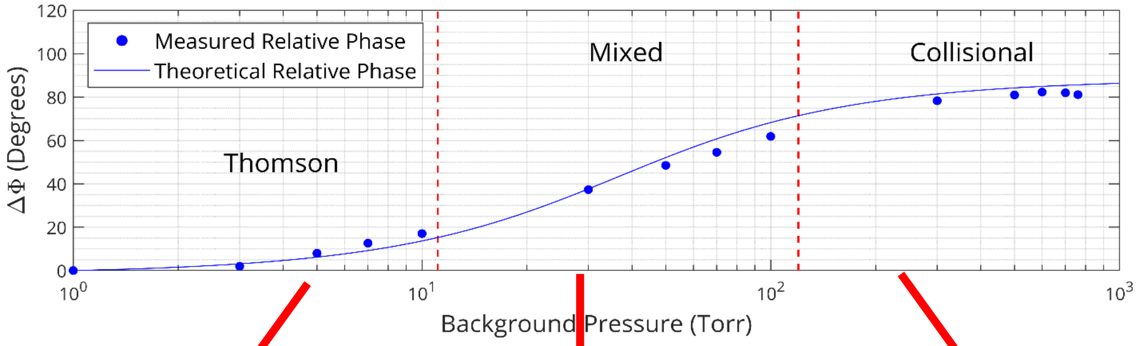

$$V_S = A\frac{e^2}{m\omega}N_e \qquad V_S = A\frac{e^2}{m\sqrt{\omega^2+\nu_m^2}} \qquad V_S = A\frac{e^2}{m\nu_m}N_e$$

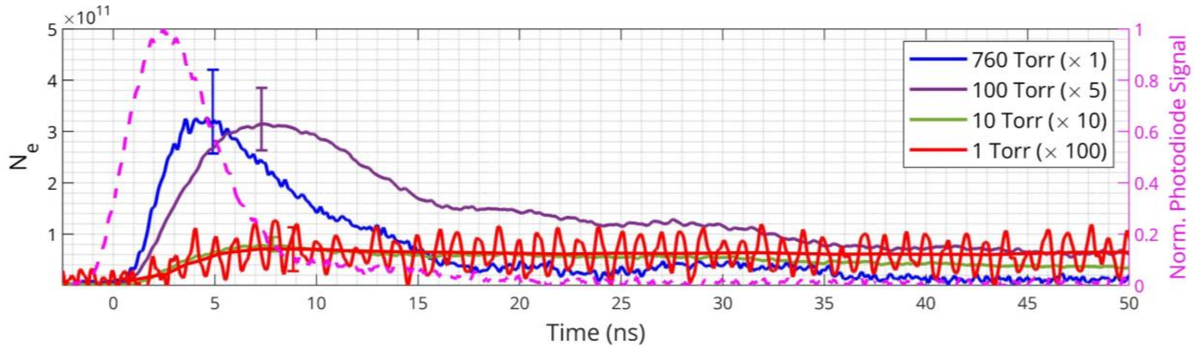

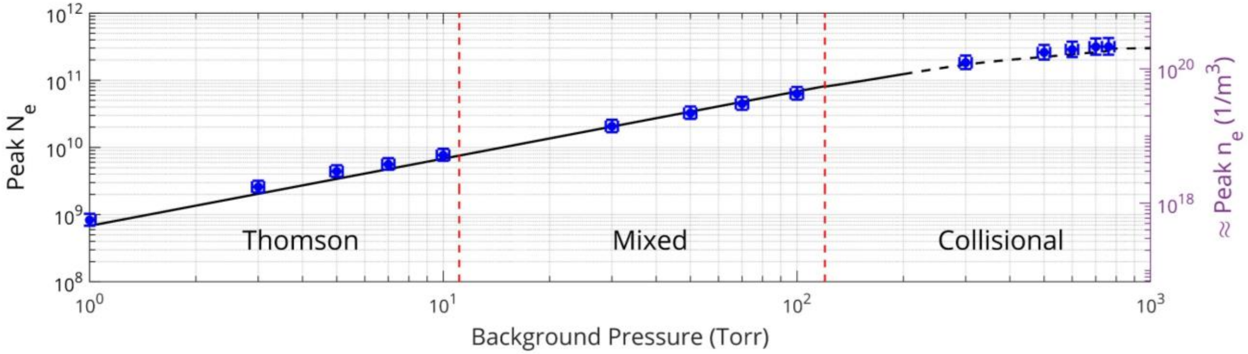

- Ideality of Thomson regime: knowledge of ν_m is unnecessary

Patel et al. *Sci. Reports* (2021)

Nanosecond Repetitively Pulsed Discharges (1 atm): CMS-LRS

LRS: Laser Rayleigh Scattering
CMS: Coherent Microwave Scattering

Applications. Important CMS features:

- Plasma-assisted ignition and combustion, aerodynamic flow control, material processing, plasma medicine
- Collisional CMS (1 atm) $V_s(t) = A\frac{e^2}{m\nu_m(t)} N_e(t)$ - knowledge of collisional frequency $\nu_m(t)$ is required
- This (in turn) requires $n_g(t)$- gas number density; σ_{eg}- e-g collision cross-section, v_{Te}-electron thermal velocity (as $\nu_m = n_g\sigma_{eg}v_{Te}$)

Experimental details:

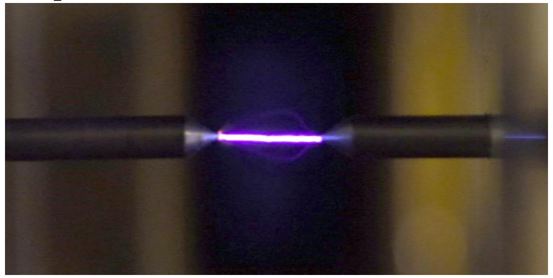

- Pin-to-pin configuration;
- 1 atm;
- HV pulse: 20kV, 100 ns, 5 mJ.

Raw decay by CMS only (unphysical):

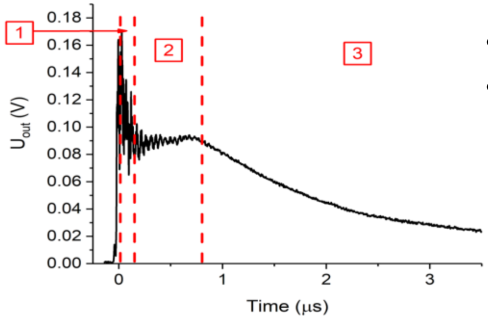

- Plateau is unphysical
- Reason: Due to simultaneous reduction of n_g and n_e

n_g measurements by LRS :

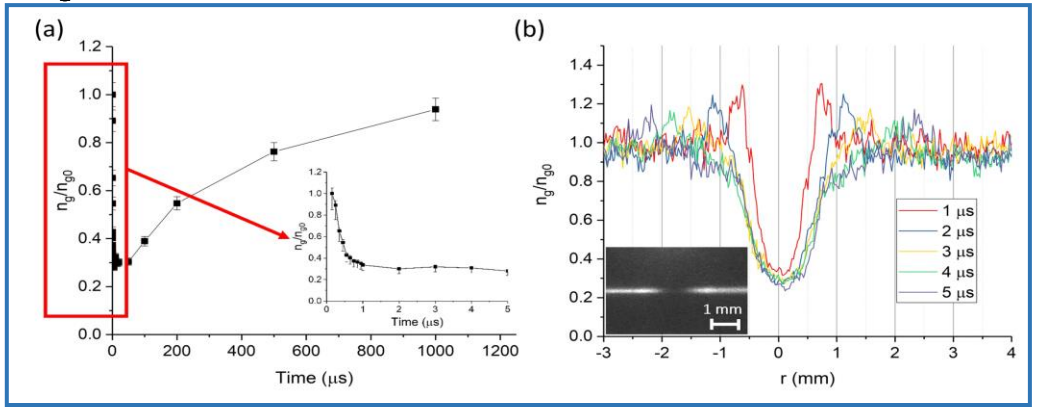

Corrected n_e decay (CMS-LRS combined):

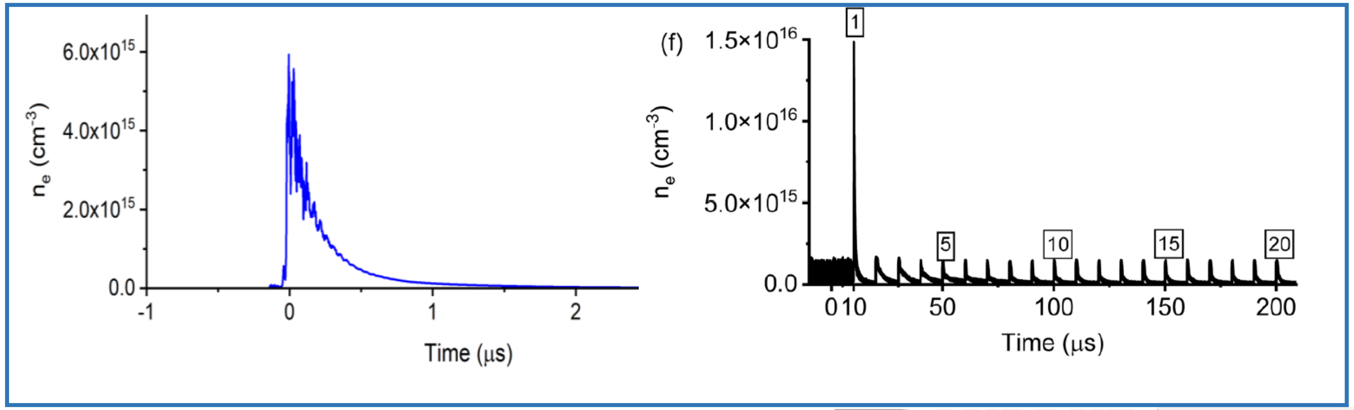

Wang et.al. *J. Appl. Phys.* (2021)

Nanosecond Repetitively Pulsed Discharges (1 atm): CMS-LRS

Experimental Details:

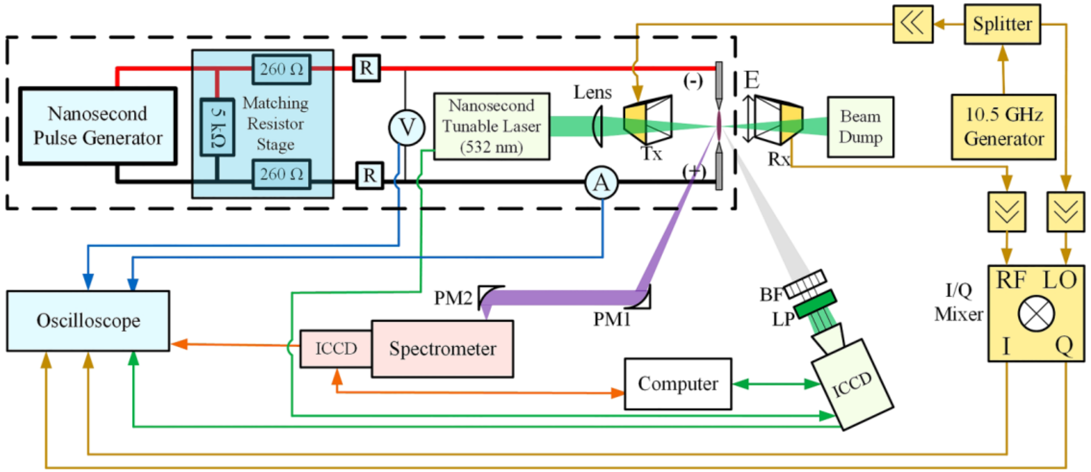

- Mechanisms of electron decay: anomalous (slow) electron decay (e.g., dissociative recombination, attachment to oxygen)
- Validation of numerical codes

During ns-pulse:

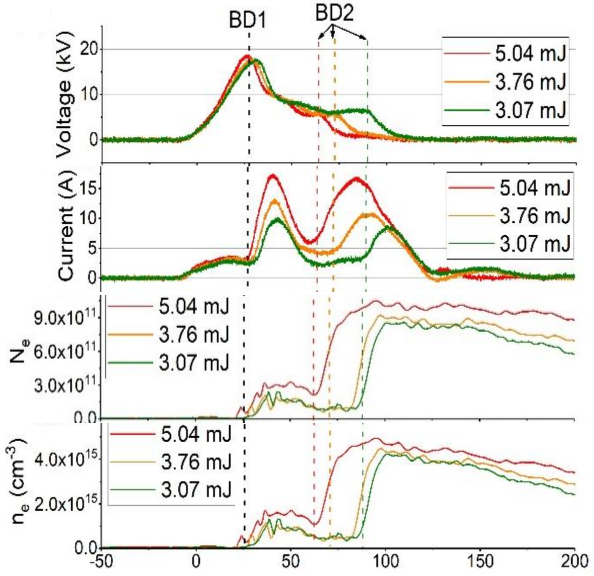

Afterglow:

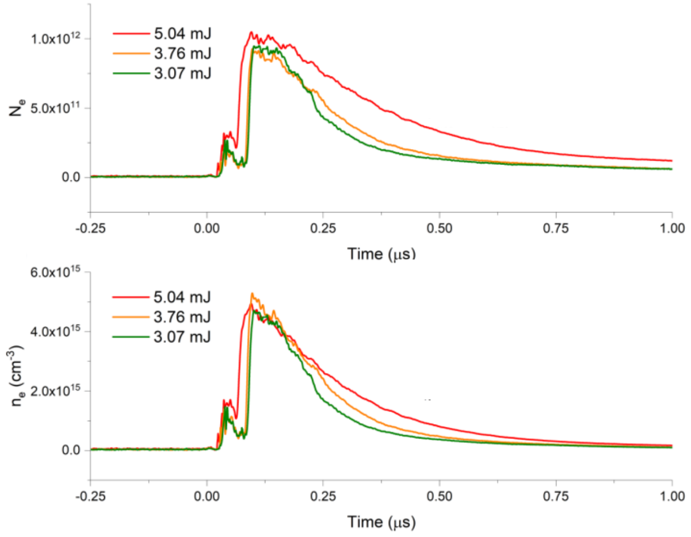

100-kHz NRP plasma dynamics:

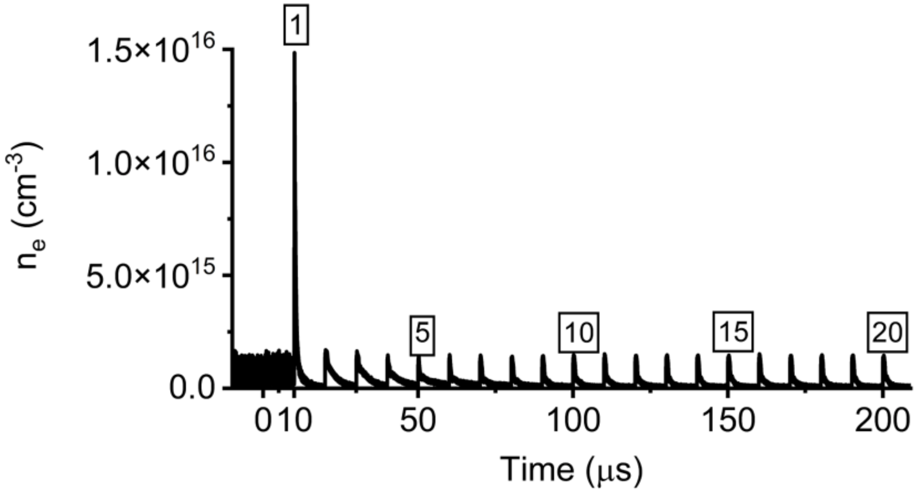

Wang et.al. *Plasma Sources Sci Technol.* (2018); Wang et.al. *J. Appl. Phys.* (2021); Wang et.al. *J. Appl. Phys.* (2022)

Glow Discharge Plasma Dynamics

Applications:

- Plasma antennae
- Plasma-based metamaterials, photonic crystals

Experimental details:

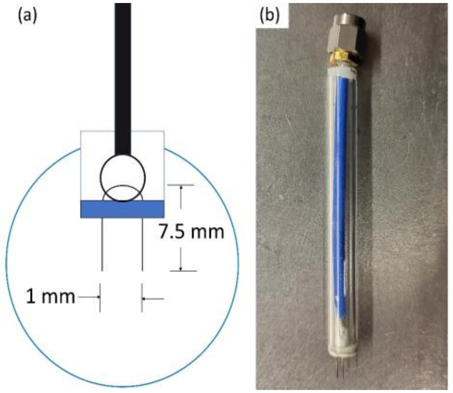

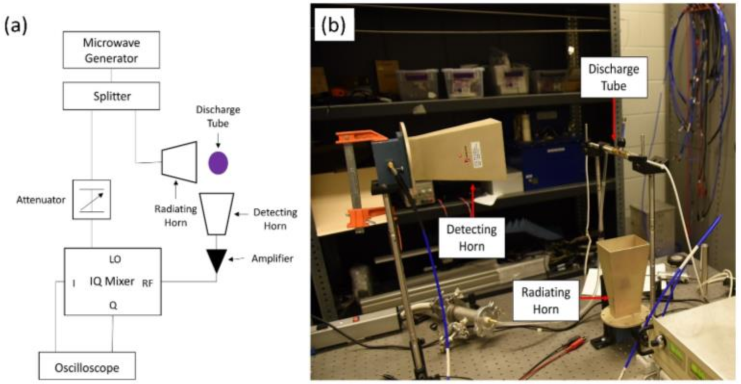

- Discharge tube: Diam-1.5 cm; Length-7 cm; 0.2-2.5 Torr
- Hairpin probe: length-7.5mm; f_0=9.8 GHz
- TMS: 3-3.9 GHz

Hairpin resonator probe:

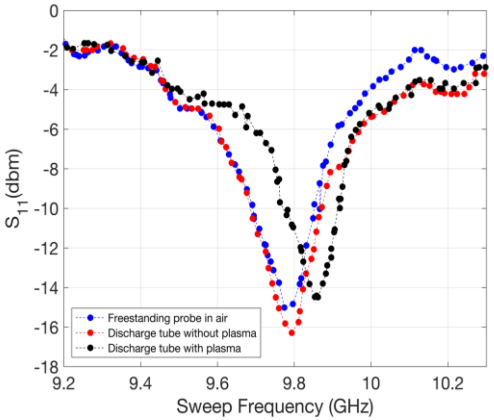

- $\omega_r^2 = \omega_o^2 + \omega_p^2$

Thomson Microwave Scattering (TMS):

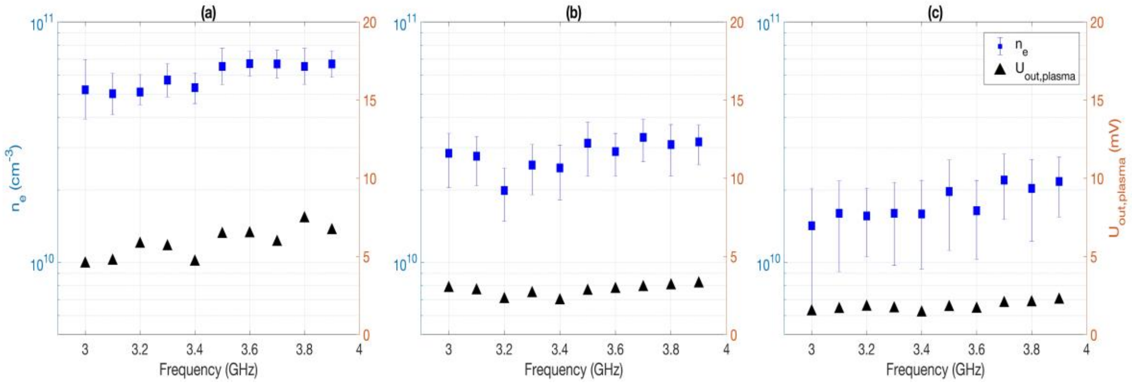

- Output signal (cross-section) is independent of frequency
- Confirms the Thomson scattering regime

TMS and Hairpin comparison:

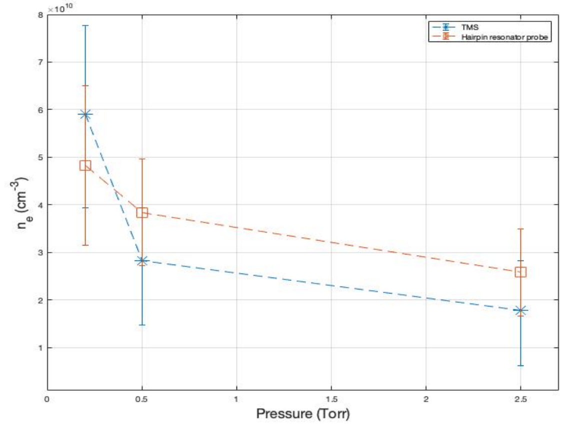

- Reasonable agreement

Ranjan et al. *Rev. Sci. Instrum.* (2022)

Outlook

1. Coherent Microwave Scattering (CMS):
   - Fundamentals and Experimental Implementation
   - Experimental Validation of the Scattering Regimes
2. Plasma dynamics and electron decay
   - Laser induced plasmas
   - Nanosecond repetitively pulsed discharges
   - Small plasma objects enclosed within glass tubes
3. Photoionization rates
   - Femtosecond photoionization at 800nm and 3.9 um
4. Electron Momentum Transfer Collision Frequency
5. Diagnostics of selective species in gaseous mixtures
   - Electric Propulsion applications
   - Combustion applications
6. Conclusions

Application and Motivation

- **Filamentation physics, combustion**
- **Direct measurements of photoionization rates at 800 nm are largely unavailable**

Laser Interferometry

- Minimal sensitivity $n_e \geq 10^{16}$ - 10^{17} cm^{-3}
- Kerr and plasma nonlinearities are significant (spatial distribution of laser intensity is unknown)
- Tunnelling ionization dominates

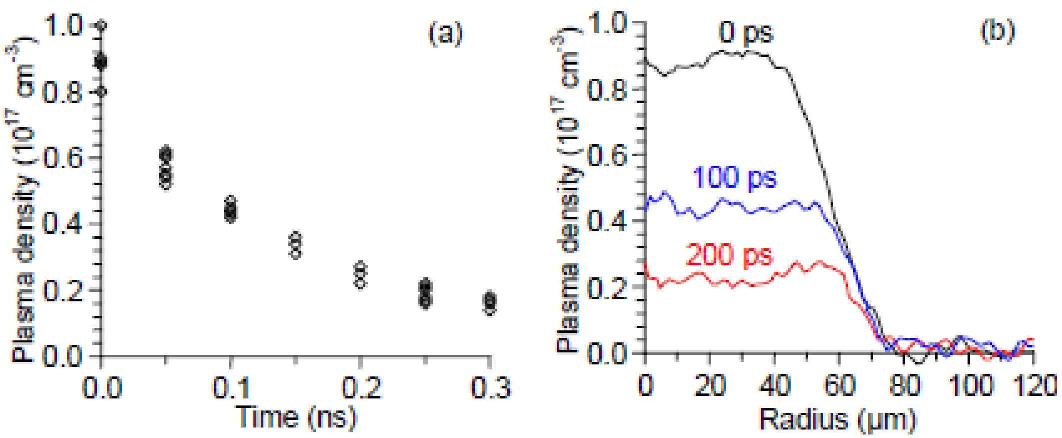

Bodrov et al. Optics Express (2011)

Time-of-flight (TOF) mass spectrometer

- Can detect signal proportional to N_e generated
- Semi-empirical method:
- Ion signal obtained cannot be calibrated (there is no testing object)
- Uses theoretical value for N_e

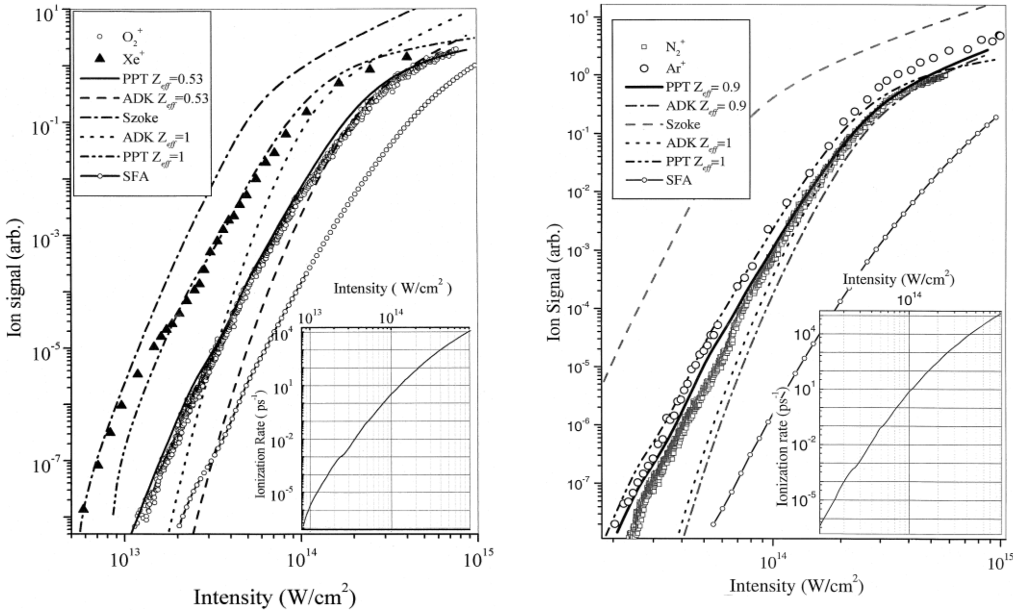

Talebpour et al. (1997) (1999)

Multiphoton ionization at 800 nm in air

Experimental details:

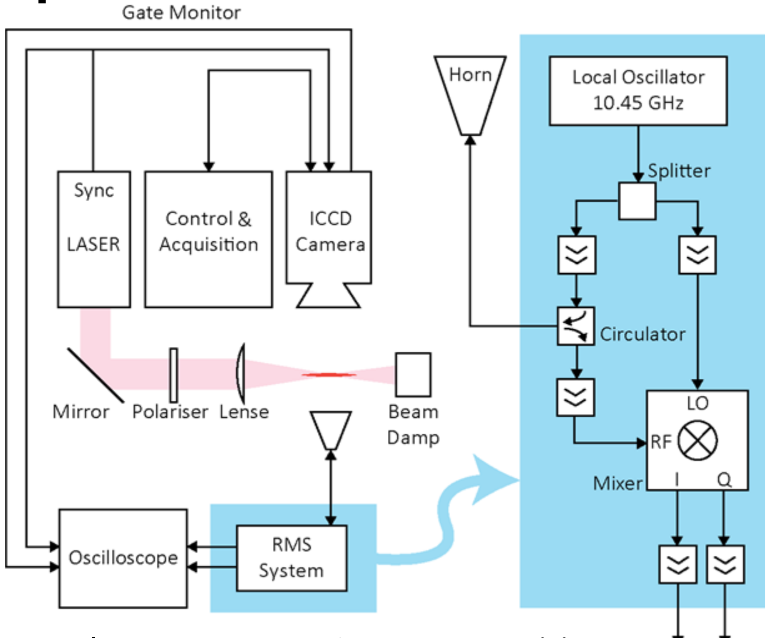

- Fs-laser: 800 nm, 100 Hz repetition rate, 0.32 – 0.78 mJ/Pulse, ~100 fs FWHM
- CMS system: 10.45 GHz, homodyne, I/Q mixer

Optical nonlinearities:

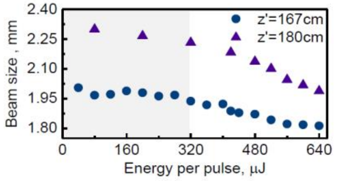

Fig. 3 Dependence of beam diameter at two locations after the focus for different beam intensities.

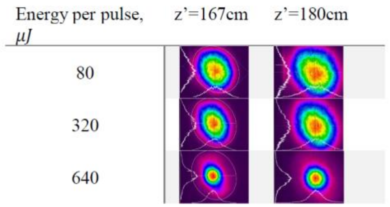

Table 1. Beam profiles at two locations after the focus

- nonlinear optical effects are OFF: can estimate Intensity in plasma

Scattering regime:

- Collisional regime: $\nu_m >> \omega$ ($\nu_m \sim 10^{12}$ s^{-1}; $\omega \sim 6 \times 10^{10}$ rad/s)
- $$V_S = \begin{cases} A \dfrac{e^2}{m\nu_m} N_e & \text{– plasma scatterer} \\ AV_D \varepsilon_0 (\varepsilon_D - 1)\omega & \text{– dielectric scatterer} \end{cases}$$

8-photon MPI of O_2:

$$N_e = \frac{231\,\pi}{1024 \cdot 16} \sqrt{\frac{\pi}{8}}\, \sigma_8\, n_0\, \tau\, \pi\, w_0^2\, z_R\, I_0^{\,8}$$

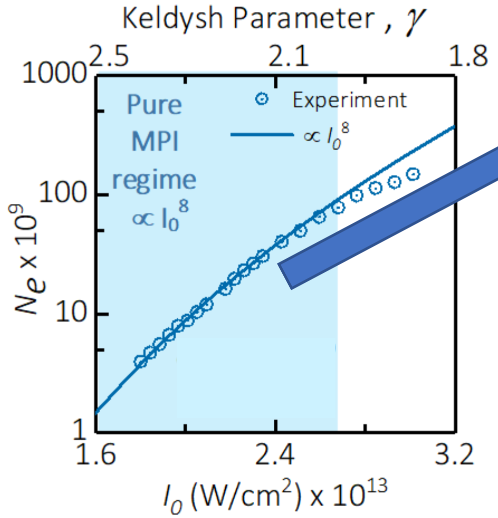

$\sigma_8 = 1.2 \times 10^{-126}$ s^{-1}W^{-1}m^{16}

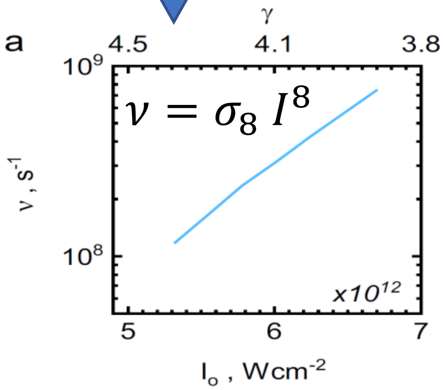

Sharma et.al. *Sci. Reports* (2018); Sharma et.al. *J. Appl. Phys* (2019)

Femtosecond Tunneling Photoionization of air at 3.9 μm

Experimental details:

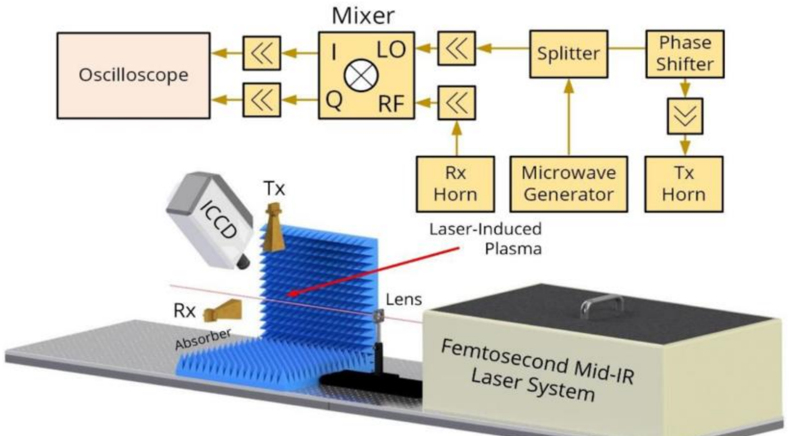

- Fs-laser (TU Wien, Austria): 3.9 μm, 30 mJ, τ_{FWHM}=117.7 fs, beam diameter ~ 4mm, 150 mm lens, beam waist radius w_0 =95.85 μm
- CMS system (Purdue, USA): 11 GHz, homodyne, I/Q mixer

Linear regime:

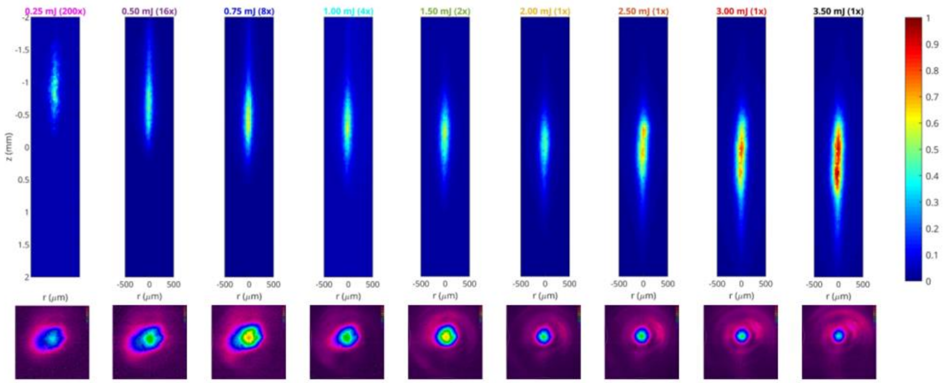

- Oblate spheroid with semi-axis estimates of $\mathfrak{a} = \mathfrak{b}$ = 100 μm and $\mathfrak{c}$ = 0.75 mm.
- Optical nonlinearities are negligible up to ~2 mJ

Photoionization rate measurements:

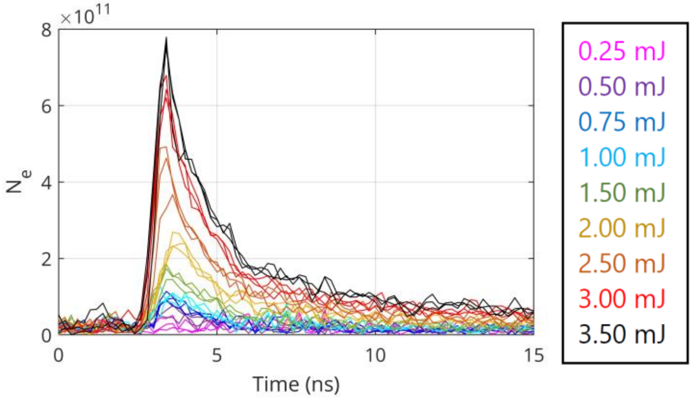

From CMS

$$n_e = \frac{N_e}{V_p}$$

From ICCD camera

2.5x10^{19} cm^{-3}

$$n_e = n_g \nu_{PI} \tau_{FWHM}$$

From SHG FROG

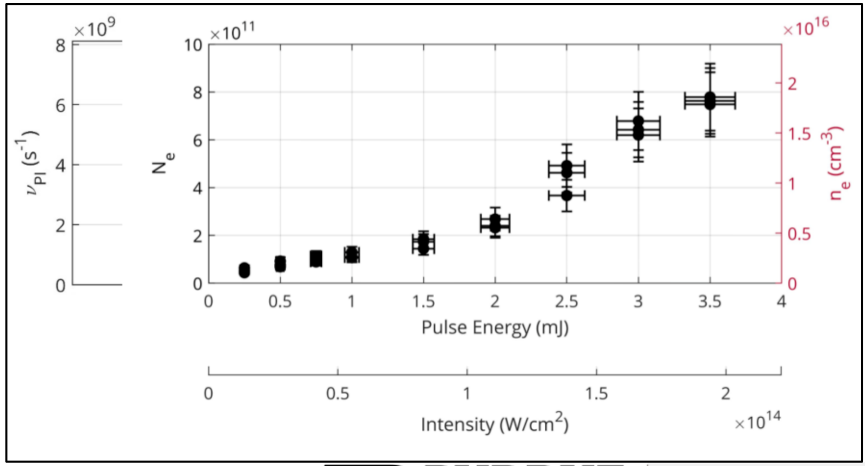

Patel et al. *Phys. Rev. E* (2022)

Photoionization rates at 800 nm

Experimental details:

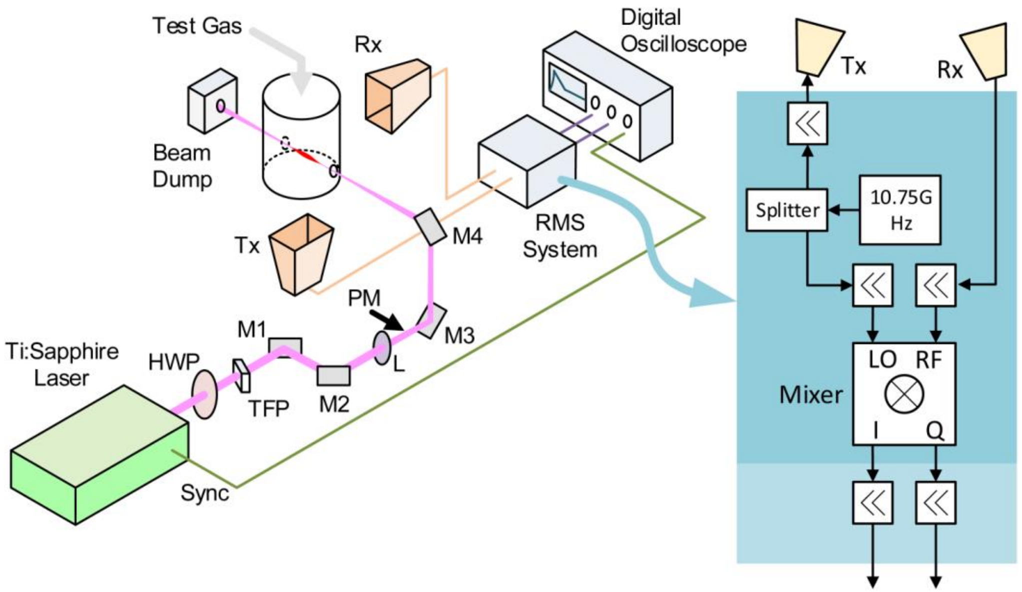

N_e measurements for variety of gases:

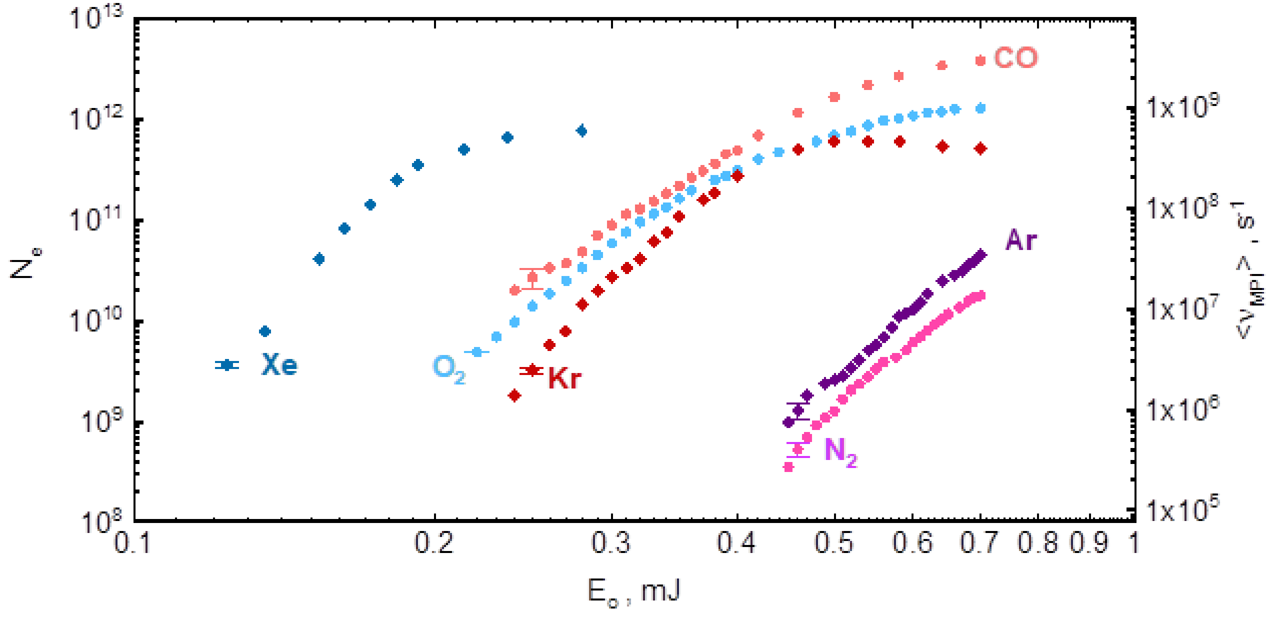

- Nonlinear optical effects are not negligible ⇒ precise intensity is unknown
- Spatially-averaged photoionization rates:

$$\langle \nu \rangle = \frac{\int \nu dV}{V_0}, \; V_0 = \frac{4}{3}\pi\, w_0^2\, z_R$$

Sharma et.al. *J. Appl. Phys* (2019)

Outlook

1. Coherent Microwave Scattering (CMS):
   - Fundamentals and Experimental Implementation
   - Experimental Validation of the Scattering Regimes
2. Plasma dynamics and electron decay
   - Laser induced plasmas
   - Nanosecond repetitively pulsed discharges
   - Small plasma objects enclosed within glass tubes
3. Photoionization rates
   - Femtosecond photoionization at 800nm and 3.9 um
4. Electron Momentum Transfer Collision Frequency
5. Diagnostics of selective species in gaseous mixtures
   - Electric Propulsion applications
   - Combustion applications
6. Conclusions

Electron Momentum-Transfer Collision Frequency Measurements

Motivation and Applications:

- Relevant for broad range of small-size plasmas: laser-initiated, NRP, etc.
- Lack of direct diagnostics of ν_m
- ν_m is hard to estimate (EEDF, local background pressure often unknow)

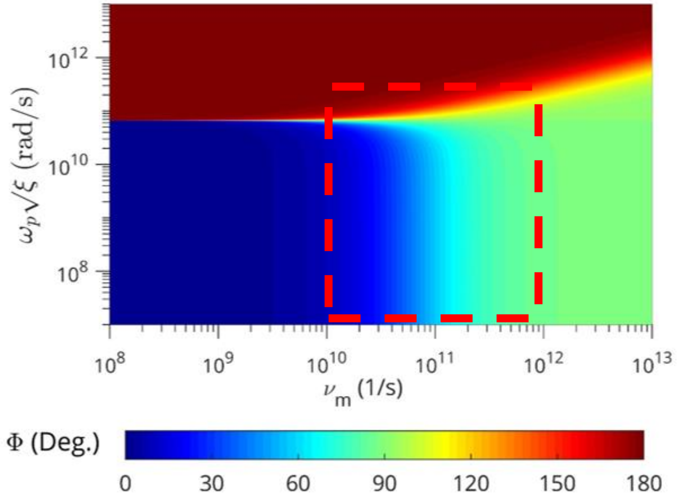

Concept:

$$\tan(\Phi) = \frac{\nu_m}{\omega} \Rightarrow \nu_m = \omega \tan(\Phi)$$

- Phase measurements can be used to directly determine ν_m
- Sensitivity in transitional region: ν_m and ω are comparable

Absolute calibration of phase measurement:

- Set Φ measured for dielectric scatterer (or at low pressure) as $\Phi = 0$
- Free electrons (Thomson): $\ddot{s} = -\frac{e}{m}E \rightarrow \dot{s} \propto i\omega E \rightarrow j \propto i\omega E$
- Dielectric bullet: $j \propto \frac{\partial P}{\partial t} \propto i\omega E$

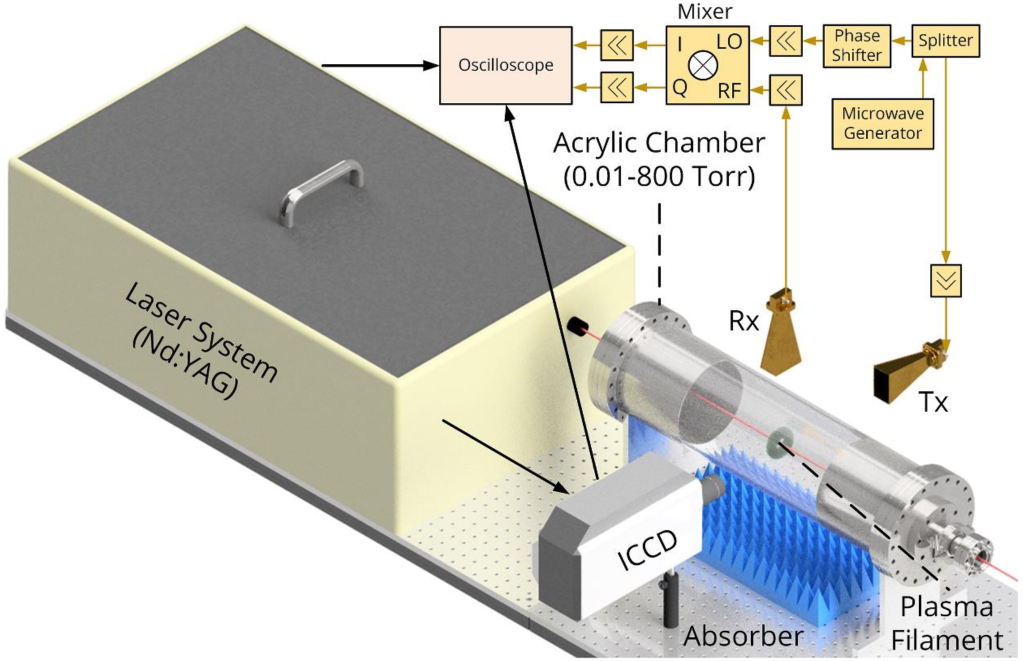

Experimental Setup:

- Oxygen: 287.5 nm (2+1) REMPI $C^3\Pi_g (v' = 2, J') \leftarrow O_2\ X^3\Sigma_g^- (v'' = 0, J'')$
- Air: 287.5 nm (2+1) REMPI $C^3\Pi_g (v' = 2, J') \leftarrow O_2\ X^3\Sigma_g^- (v'' = 0, J'')$
- Krypton: 212.5 nm $Kr\ 5p[1/2]_0 \leftarrow Kr\ 4p^6(^1S_0)$

Electron Momentum-Transfer Collision Frequency (via Phase Measurements)

ν_m-measurements (2+1 REMPI of Oxygen at 287.5 nm, 100 Torr):

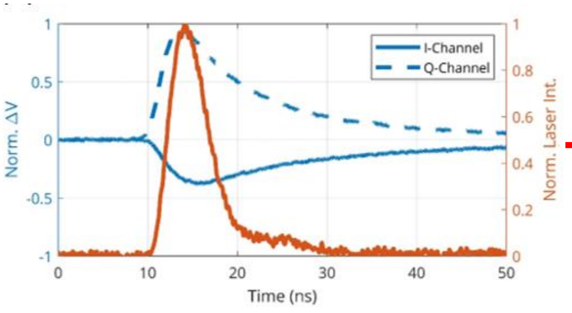

Retrieve $\Delta\Phi_S$ and V_S

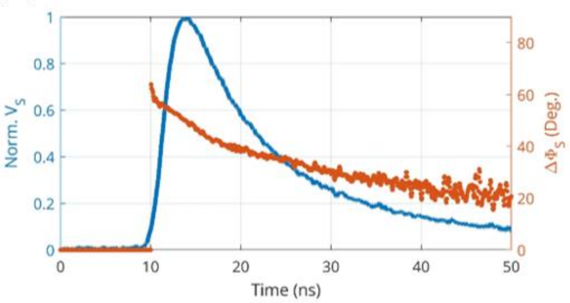

Infer ν_m

$\nu_m = \omega \tan(\Phi)$

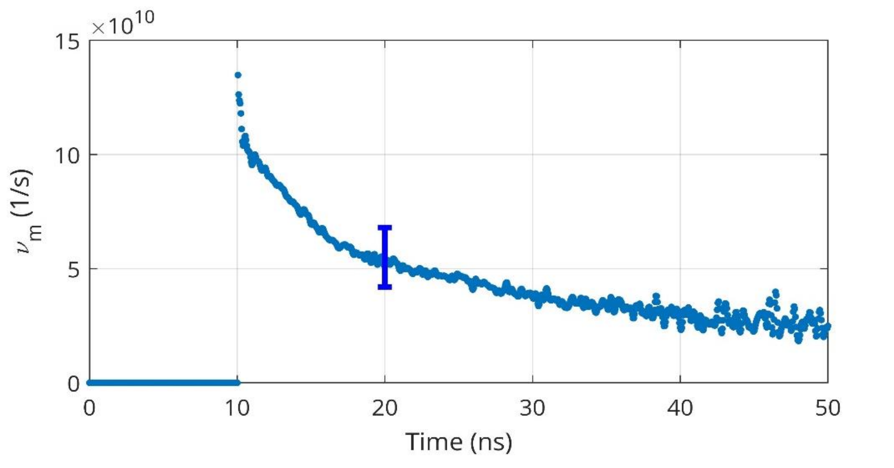

Various pressures:

Oxygen

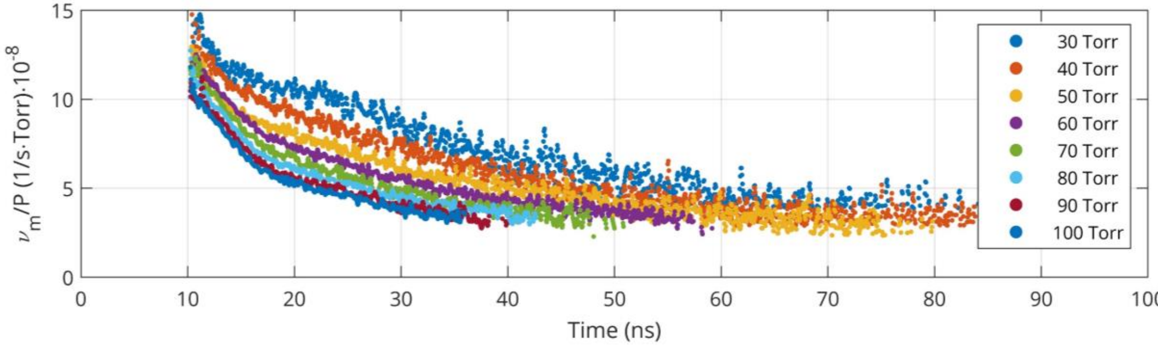

Air

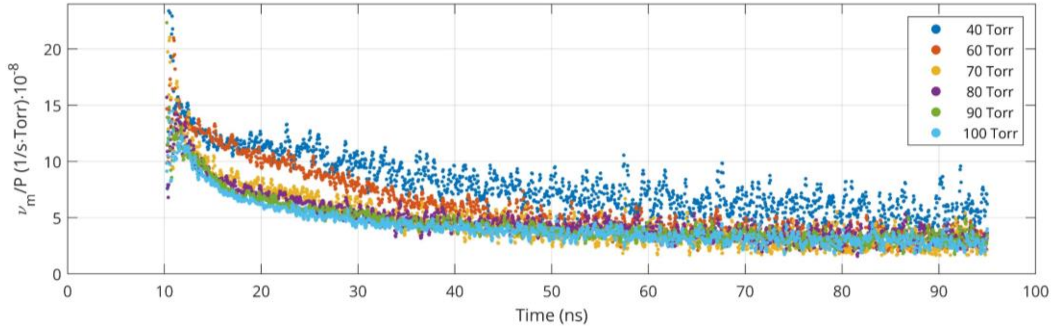

- Enables direct measurement of collision frequency ν_m (for actual Electron Energy Distribution Function in plasma object under test)

Patel et al. *Plasma Sources Sci. Technol.* (2022)

T_e via Phase Measurement

Cross-section (tabulated)

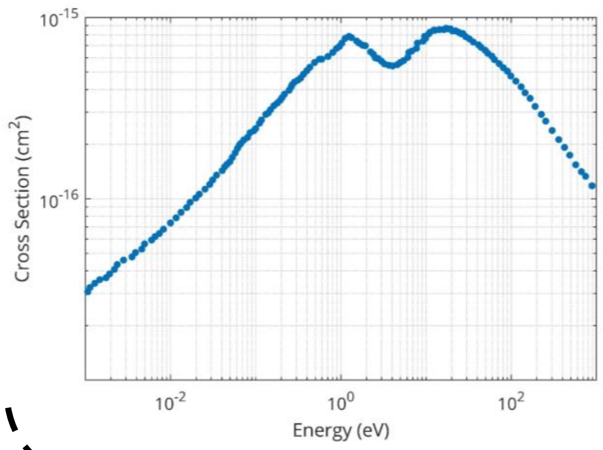

ν_m-measurement

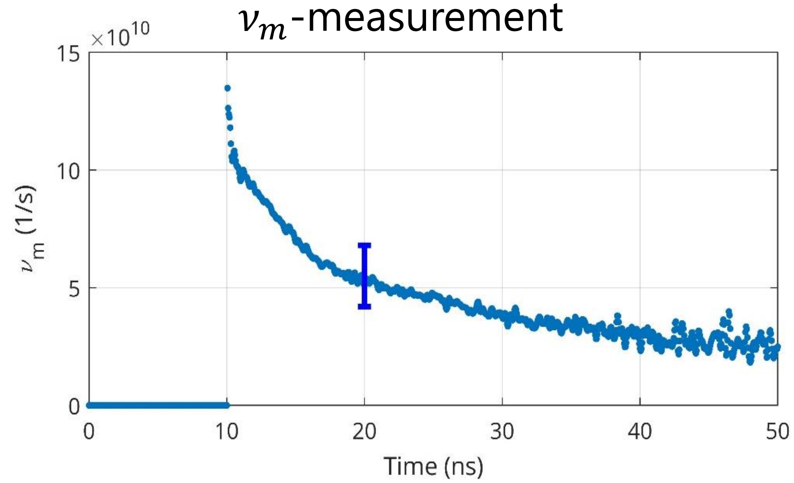

Associate T_e (or ϵ_e) $\nu_m = n_{O_2} \langle v \sigma_{tr,e-O_2}(\epsilon) \rangle$

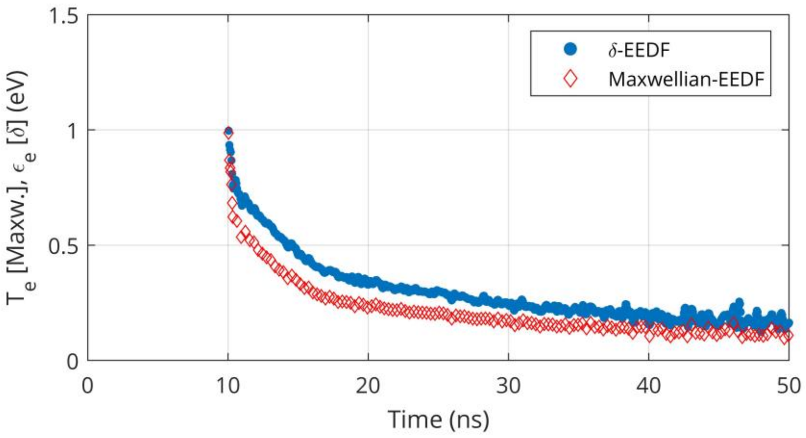

- Measured ν_m can be used to derive T_e

Patel et al. *Plasma Sources Sci. Technol.* (2022)

Use of Phase Measurement for accurate evaluation of N_e

ν_m-measurement

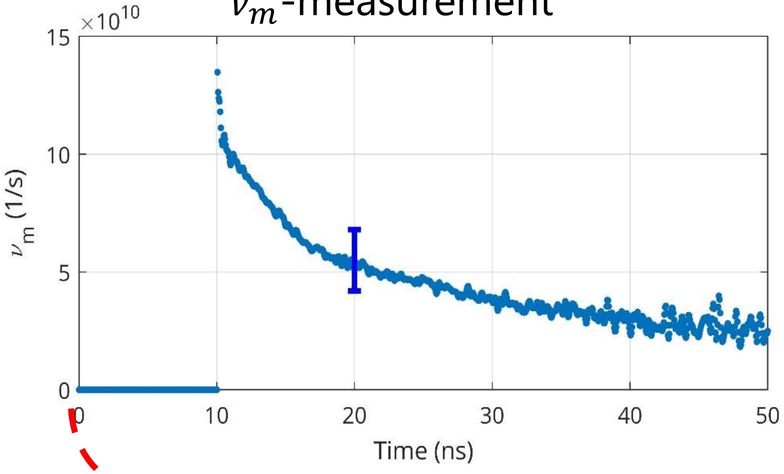

V_s-measurement

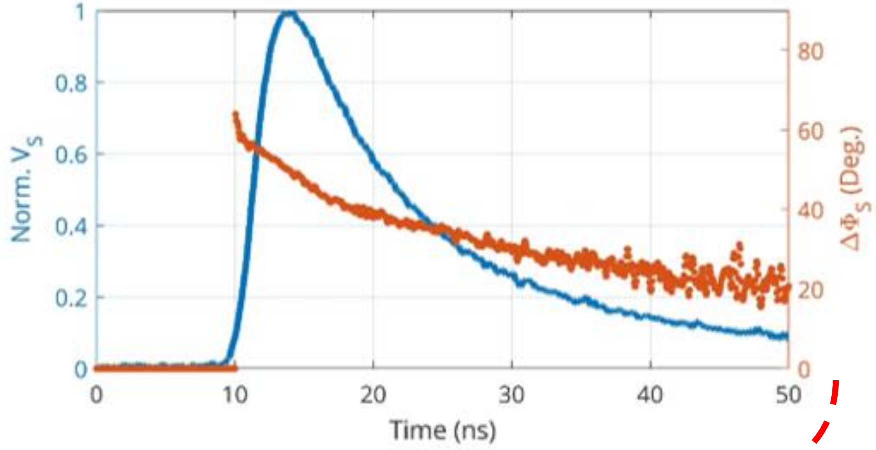

Derive N_e

$$V_s = A \frac{e^2}{m\sqrt{\omega^2 + \nu_m^2}} N_e$$

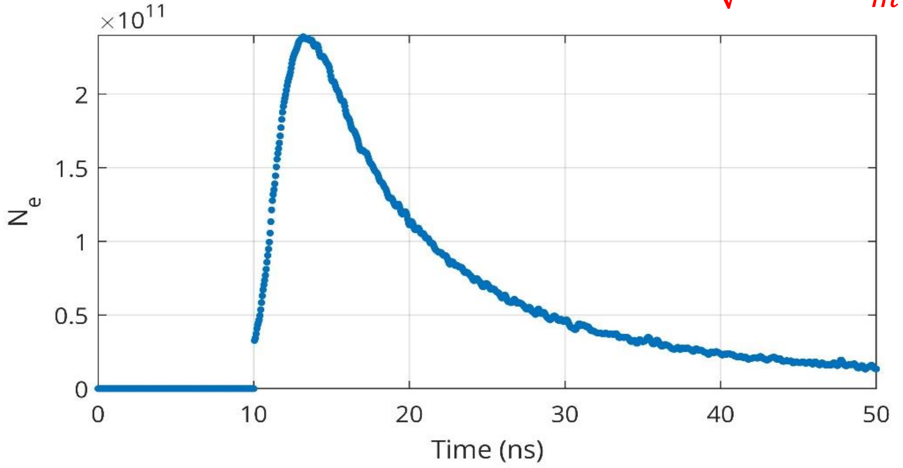

Patel et al. *Plasma Sources Sci. Technol.* (2022)

Outlook

1. Coherent Microwave Scattering (CMS):
   - Fundamentals and Experimental Implementation
   - Experimental Validation of the Scattering Regimes
2. Plasma dynamics and electron decay
   - Laser induced plasmas
   - Nanosecond repetitively pulsed discharges
   - Small plasma objects enclosed within glass tubes
3. Photoionization rates
   - Femtosecond photoionization at 800nm and 3.9 um
4. Electron Momentum Transfer Collision Frequency
5. Diagnostics of selective species in gaseous mixtures
   - Electric Propulsion applications
   - Combustion applications
6. Conclusions

Diagnostics of gaseous species in Electric Propulsion devices

Experimental Details:

KDC-40 gridded ion accelerator and REMPI-TMS diagnostics

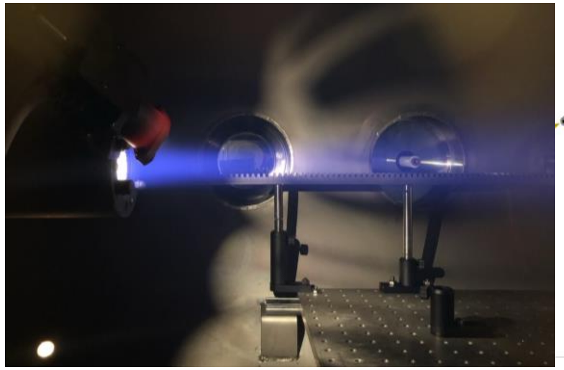

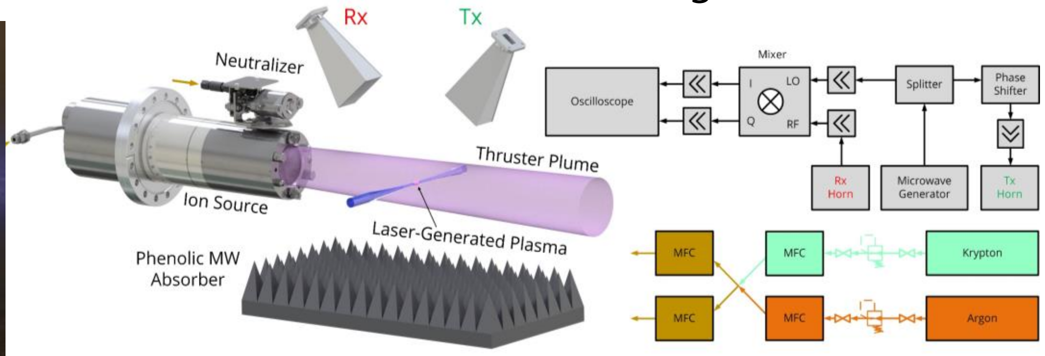

REMPI-TMS (radar REMPI) concept:

- Ionize selective component by REMPI
- Use TMS to detect REMPI-induced electrons
- Correlate TMS measurement to number density of original specie (via absolute calibration)

(2+1) 212.5 nm REMPI of neutral Krypton

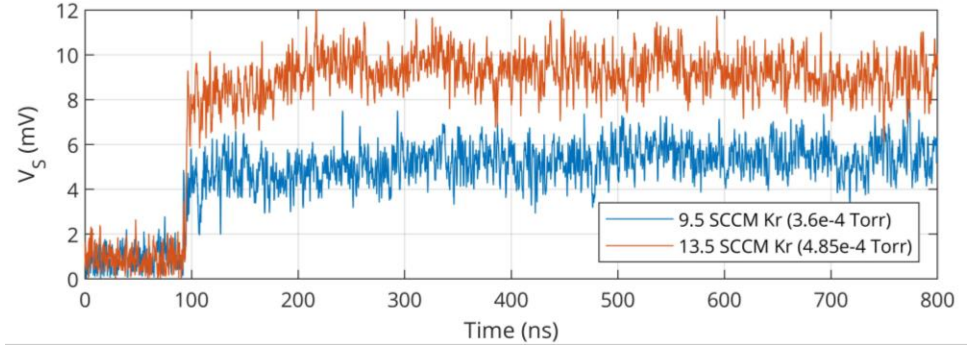

(3+2) 214nm REMPI of singly-ionized Krypton

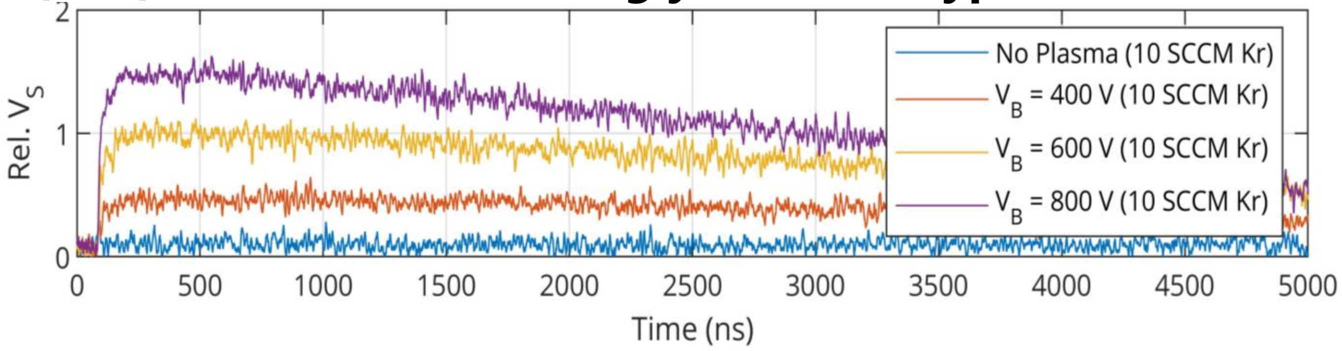

- Detection on neutral and singly-ionized Krypton is feasible
- Sensitivity is high (down to ~10^{11} cm^{-3})

Patel et al. *Under review* (2022)

Diagnostics of gaseous species in Combustion

Experimental system schematics:

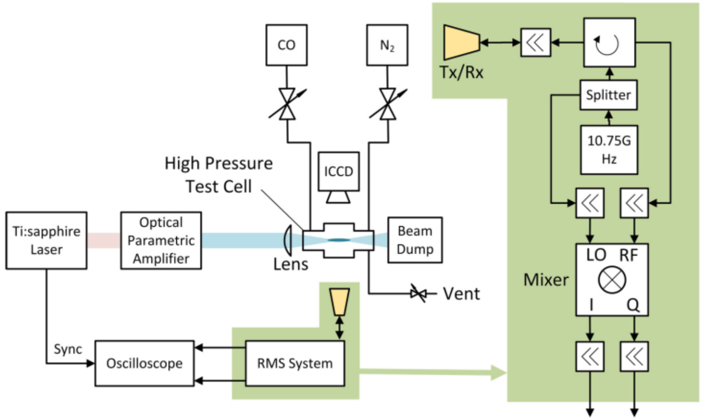

(2+1) REMPI of CO at 230.1 nm:

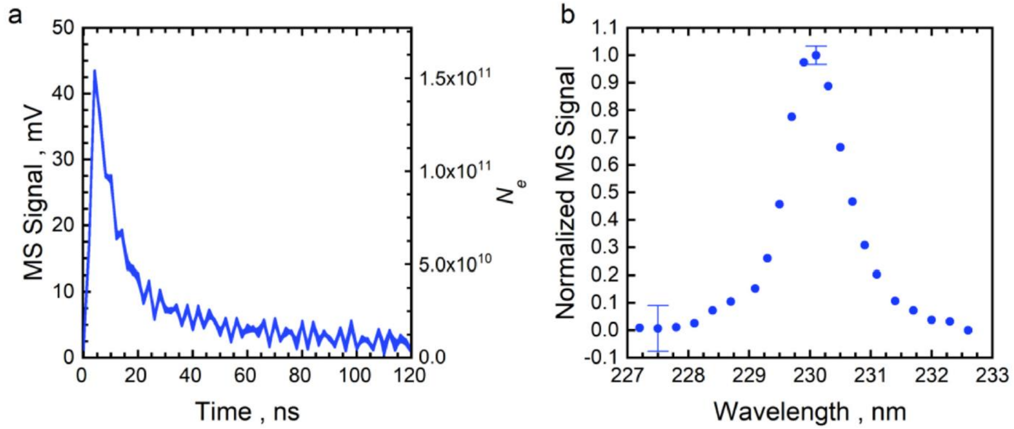

CO number density diagnostics in gaseous mixture (concept):

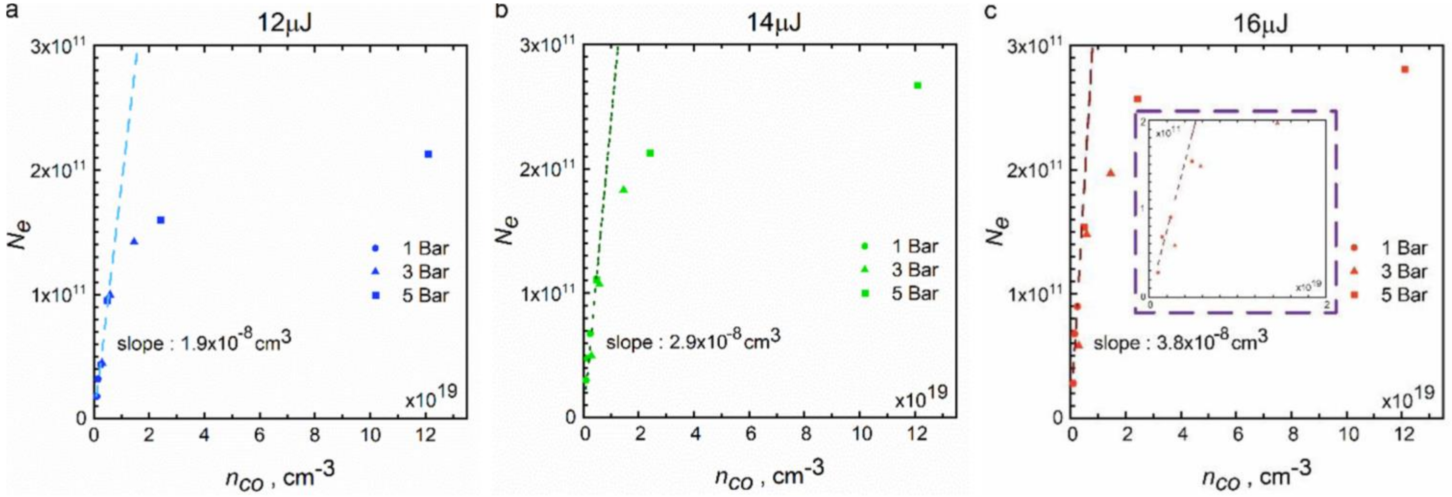

- Number of REMPI-induced electrons scales linearly with n_{CO}
- Independent of the buffer gas pressure up to 5 bar
- Saturation is due to laser beam energy (two-photon absorption/photoionization)

Sharma et.al. *J. Appl. Phys.* (2020)

Conclusions

- Coherent Microwave Scattering (CMS) is powerful tool for diagnostics of miniature plasma objects
    - High sensitivity due to in-phase coherency: $\langle P_S \rangle \propto N_e^2$ (not $\langle P_S \rangle \propto N_e$ as for incoherent counterpart)
    - Thomson scattering regime at low pressures: Ideality of Thomson regime (independent of ν_m)
    - Temporally-resolved measurements of plasma dynamics
    - Tabulation of photoionization rates
    - Direct measurements of ν_m in intermediate Collisional-Thomson regime
- Applications of in-phase Coherent Microwave Scattering:
    - Laser-induced plasmas
    - Nanosecond Repetitively Pulsed discharges
    - Small-size glow discharges
    - Electric propulsion and Combustion

Acknowledgements:

This work was supported by NSF/DOE Partnership in the Basic Plasma Science and Engineering program (Grant No. 1465061) and U.S. Department of Energy (Grant No. DE-SC0018156; Grant No. DE-SC0023209).

References:

1. A. Patel, C. Gollner, R. Jutas, V. Shumakova, M.N. Shneider, A. Pugzlys, A. Baltuska, and A. Shashurin "Ionization rate and plasma dynamics at 3.9-micron femtosecond photoionization of air" Phys. Rev. E (2022).
2. A. Ranjan, A. Patel, X. Wang, and A. Shashurin "Thomson microwave scattering for diagnostics of small plasma objects enclosed within glass tubes" Rev. Sci. Reports (2022).
3. A.R. Patel, X. Wang, E.L. Braun, A. Ranjan, M.N. Slipchenko, S. Macheret, M.N. Shneider, and A. Shashurin "Electron Momentum-Transfer Collision Frequency Measurements in Small Plasma Objects Via Coherent Microwave Scattering" Palsma Source Sci. Technol. (2022).
4. A.R. Patel, S.L.B. Karunarathne, N. Babusis, and A. Shashurin "The Application of Coherent Microwave Scattering and Multiphoton Ionization for Diagnostics of Electric Propulsion Systems" Under review (2022).
5. X. Wang, A. Patel, and A. Shashurin "Initial transient stage of pin-to-pin nanosecond repetitively pulsed discharges in air" J. Appl. Phys. **132**, 013301 (2022).
6. A. Patel, A. Ranjan, X. Wang, M.N. Slipchenko, M.N. Shneider, and A. Shashurin "Thomson and collisional regimes of in-phase coherent microwave scattering off gaseous microplasmas" Sci. Reports **11**, 23389 (2021).
7. X. Wang, A. Patel, S. Bane, and A. Shashurin "Experimental study of atmospheric pressure single-pulse nanosecond discharge in pin-to-pin configuration" J. Appl. Phys. **130**, 103303 (2021).
8. X. Wang, A. Patel, and A. Shashurin "Combined microwave and laser Rayleigh scattering diagnostics for pin-to-pin nanosecond discharges" *J. Appl. Phys.* **129**, 183302 (2021)
9. A. Sharma, E. L. Braun, A. R. Patel, K. A. Rahman, M. N. Slipchenko, M. N. Shneider, and A. Shashurin "Diagnostics of CO concentration in gaseous mixtures at elevated pressures by Resonance Enhanced Multi-Photon Ionization and Microwave Scattering" *J. Appl. Phys.* **128**, 141301 (2020).
10. A. Sharma, M.N. Slipchenko, M.N. Shneider, K.A. Rahman, and A. Shashurin "Direct measurement of electron numbers created at near-infrared laser-induced ionization of various gases" *J. Appl. Phys.* **125,** 193301 (2019).
11. X. Wang, P. Stockett, R. Jagannath, S. Bane, and A. Shashurin "Time-Resolved Measurements of Electron Density in Nanosecond Pulsed Plasmas Using Microwave Scattering" *Plasma Sources Sci. Technol.* **27**, 07LT02 (2018).
12. A. Sharma, M.N. Slipchenko, M.N. Shneider, X. Wang, K.A. Rahman, and A. Shashurin "Counting the electrons in a multiphoton ionization by elastic scattering of microwaves" *Sci. Reports* **8**, 2874 (2018).

Thank you!

Approach: 8-photon MPI of Oxygen

- Integrate over beam waist/plasma area:

$$n_e = n_0 \tau \sqrt{\frac{\pi}{8}} \sigma_8 \, I^8 \quad \Longrightarrow \quad N_e = \sigma_8 \, n_0 \tau \sqrt{\frac{\pi}{8}} \int I^8 dV$$

(For Gaussian pulse in time domain)

N_e: Measure using CMS

$n_0 \tau \sqrt{\frac{\pi}{8}} \int I^8 dV$: Known/measurable quantities

- If nonlinear optical effects are negligible:

$$I(r,z) = I_0 \frac{w_0^2}{w(z)^2} e^{-\frac{2r^2}{w(z)^2}} \quad \Longrightarrow \quad \int I(\mathbf{r})^8 dV = \frac{231\,\pi}{1024 \cdot 16} {I_0}^8 \, \pi \, w_0^2 \, z_R$$

- Finally:

$$N_e = \frac{231\,\pi}{1024 \cdot 16} \sqrt{\frac{\pi}{8}} \sigma_8 \, n_0 \, \tau \, \pi \, w_0^2 \, z_R \, {I_0}^8 \quad \Longrightarrow \quad \text{Find } \sigma_8$$

Linear operation regime

- Non- linear refractive index: $n = n_0 + n_2 I - \frac{\omega_p^2}{2\omega_0^2}$
  - n_0- linear index of refraction (air)
  - Optical Kerr effect: n_2- Kerr nonlinear index coefficient
  - Plasma nonlinearity: $\omega_p^2 = \frac{e^2 n_e}{\varepsilon_0 m_e}$ - plasma frequency; ω_0 - laser frequency

- Measurements to determine onset of nonlinear optical effects:

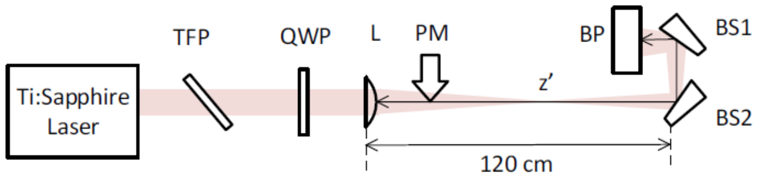

Fig. 2 The Kerr effect was examined by taking beam profiler measurements using beam profile(BP) located at distance z=167cm,180cm. for different beam intensities. A pair of wedge beam samplers (BS) were used to reduce the intensity of the beam after focus to prevent saturation of BP.

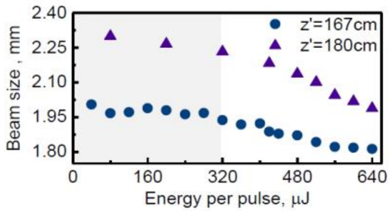

Fig. 3 Dependence of beam diameter at two locations after the focus for different beam intensities.

Energy per pulse, µJ	z'=167cm	z'=180cm
80		
320		
640		

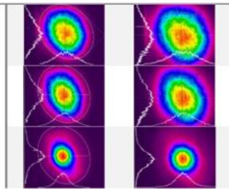

Table 1. Beam profiles at two locations after the focus

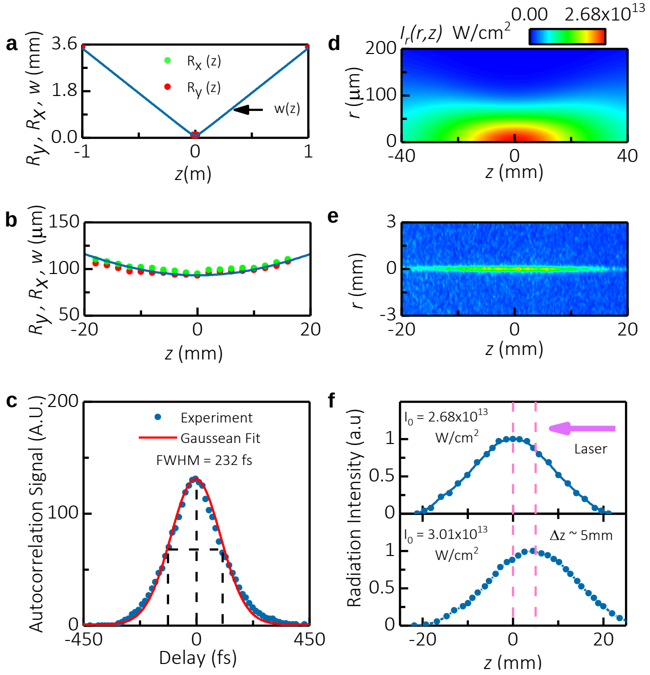

Pure linear regime was observed for laser pulse energy <320 µJ

Previous applications of CMS

Nanosecond Repetitive Pulsed Discharges

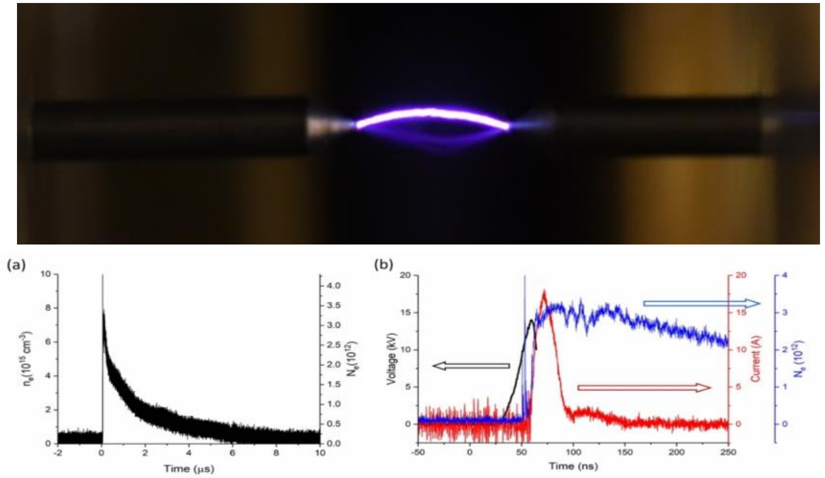

Wang et al *Plasma Sources Sci. Technol.* 2018

Laser Induced Plasmas

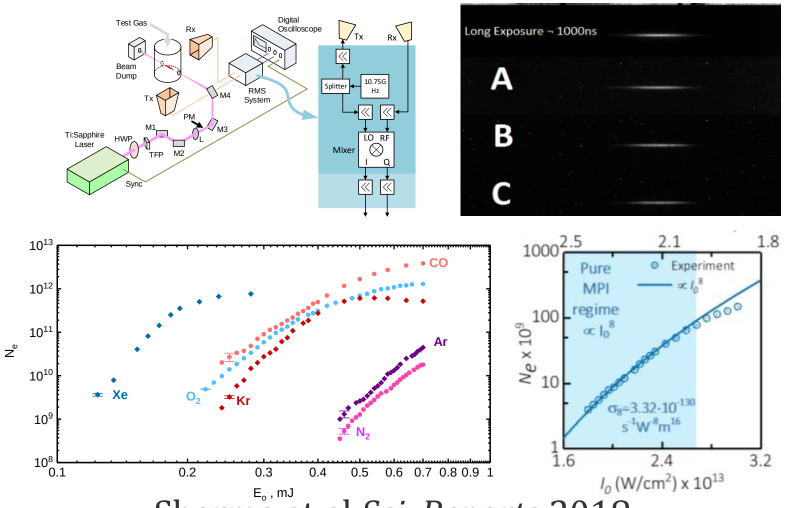

Sharma et al *Sci. Reports* 2018

Electrosurgical Discharges

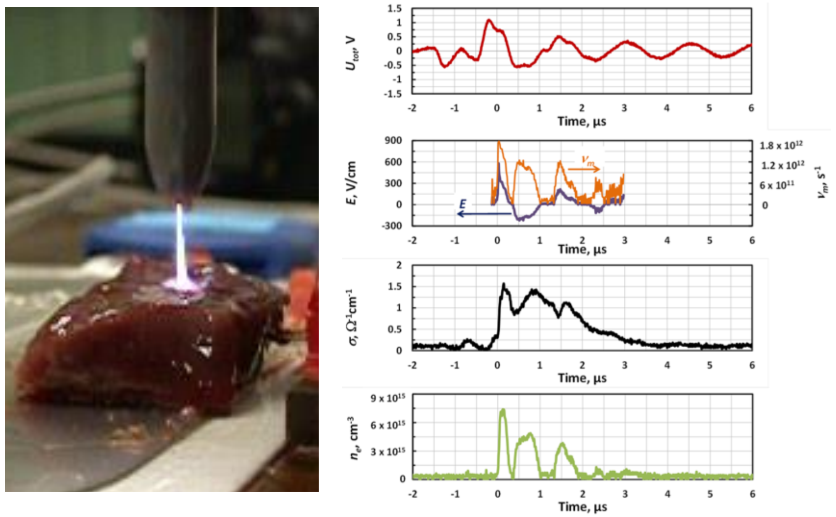

Shashurin, Canady et al *Sci. Rep.* 2015

Atmospheric-Pressure Plasma Jets

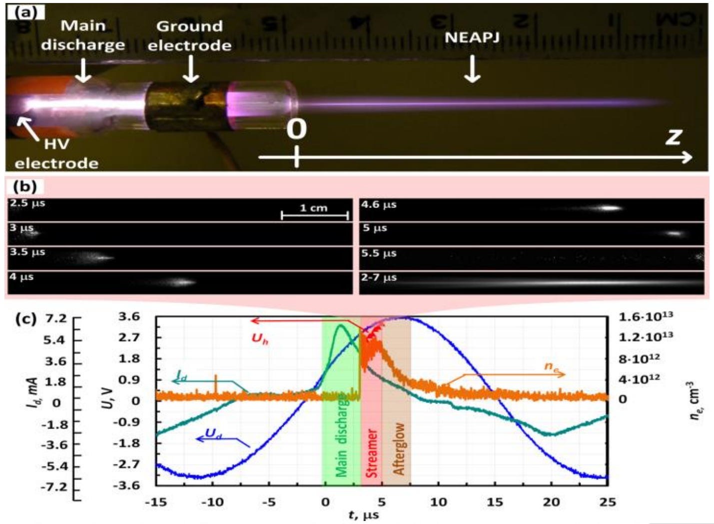

Shashurin, Keidar et al *Appl Phys Lett.* 2010